Charles University

Faculty of Pharmacy in Hradec Králové

Department of Pharmaceutical Chemistry and Pharmaceutical Analysis

University of Helsinki

Faculty of Pharmacy

Division of Pharmaceutical Chemistry and Technology

Synthesis of aerothionin analogs as potential antimycobacterial agents

diploma thesis

Martina Šimovičová

Supervisors: doc. PharmDr. Jan Zitko, Ph.D.; Adjunct Prof. Paula Kiuru, Ph.D.

Helsinki, Finland 2021

Author’s Declaration:

„I declare that this thesis is my original author's work, which has been composed solely by myself (under the guidance of my consultant). All the literature and other resources from which I drew information are cited in the list of used literature and are quoted in the paper. The work has not been used to get another or the same title.“

Martina Šimovičová

Hradec Králové, August 2021

ACKNOWLEDGEMENT

I would like to express my sincere gratitude to my supervisors, Adjunct Prof. Paula Kiuru, Ph.D. and Assoc. Prof. PharmDr. Jan Zitko, Ph.D. for their patient guidance and useful critique and advice during the research and writing the thesis.

My great appreciation belongs to Fiammetta Vitulano, Antti Lehtinen, Katia Sirna, Riccardo Provenzani and Martin Juhás for always helping and supporting me whenever I had a question or ran into a trouble spot.

Finally, I would like to thank my friends and family for their motivation and encouragement.

This work was supported by the Ministry of Education, Youth and Sports of the Czech Republic (project SVV 260 547).

TABLE OF CONTENTS

1 LIST OF ABBREVIATIONS

AIDS	acquired immune deficiency syndrome
anh.	anhydrous
ATCC	American Type Culture Collection
ATP	adenosine triphosphate
1,3-DAP	1,3-diaminopropane
1,4-DAB	1,4-diaminobutane
BCG	bacille Calmette-Guérin (vaccine)
Boc	*tert*-butoxycarbonyl
BOP	benzotriazol-1-yl-oxy-tris-(dimethylamino)-phosphonium hexafluorophosphate
CAS	Chemical Abstracts Service (number)
CFU	colony forming unit(s)
COSY	^{1}H-^{1}H Correlation Spectroscopy
DCC	dicyclohexylcarbodiimide
DCM	dichloromethane
DCU	*N,N'*-dicyclohexylurea
DIC	diisopropylcarbodiimide
DIPEA	*N,N*-diisopropylethylamine
DMAP	4-dimethylaminopyridine
DMF	dimethylformamide
DMSO	dimethylsulfoxide
EDC·HCl	1-ethyl-3-(3-dimethylaminopropyl)carbodiimide hydrochloride
e.g.	exempli gratia (for example)

et al.	et alia (and others)
etc.	et cetera
EtOAc	ethyl acetate
GSK	GlaxoSmithKline
HATU	1-[bis(dimethylamino)methylene]-1*H*-1,2,3-triazolo[4,5-b]pyridinium 3-oxide hexafluorophosphate
HBTU	*O*-(1*H*-benzotriazol-1-yl)-*N,N,N′,N′*-tetramethyluronium hexafluorophosphate
HIV	human immunodeficiency virus
HMPA	hexamethylphosphoric triamide
HOAt	1-hydroxy-7-azabenzotriazole
HOBt	1-hydroxy-1*H*-benzotriazole
HRMS	high resolution mass spectrometry
HMBC	^{1}H-^{13}C Heteronuclear Multiple Bond Correlation Spectroscopy
HSQC	^{1}H-^{13}C Heteronuclear Single Quantum Coherence Spectroscopy
IPT	isoniazid preventive therapy
IR	infrared spectroscopy
LC-MS	liquid chromatography-mass spectrometry
LRMS	low resolution mass spectrometry
MDK (assay)	minimum duration for killing (assay)
MDR TB	multidrug-resistant tuberculosis
MeOH	methanol
MIC	minimum inhibitory concentration
MmpL3	Mycobacterial membrane protein large 3
Mtb	*Mycobacterium tuberculosis*

N-Boc-1,4-DAB	*N*-Boc-1,4-diaminobutane
N-Boc-1,3-DAP	*N*-Boc-1,3-diaminopropane
NBS	*N*-bromosuccinimide
NMR	nuclear magnetic resonance
PIDA	phenyliodine bis(trifluoroacetate)
PyAOP	(7-azabenzotriazol-1-yloxy)-tripyrrolidinophosphonium hexafluorophosphate
PyBOP	benzotriazol-1-yloxytripyrrolidinophosphonium hexafluorophosphate
r.t.	room temperature
SCX	strong cationic exchange (column)
TATU	*O*-(7-azabenzotriazol-1-yl)-*N,N,N′,N′*-tetramethyluronium tetrafluoroborate
TBTU	2-(1*H*-Benzotriazole-1-yl)-1,1,3,3-tetramethylaminium tetrafluoroborate
TB	tuberculosis
TFA	trifluoroacetic acid
TLC	thin-layer chromatography
UV	ultraviolet-visible spectroscopy
XDR TB	extensively drug-resistant tuberculosis

2 ABSTRACT (ENGLISH)

Charles University

Faculty of Pharmacy in Hradec Králové

Department of Pharmaceutical Chemistry and Pharmaceutical Analysis

Author: Martina Šimovičová

Supervisors: Assoc. Prof. PharmDr. Jan Zitko, Ph.D.; Adjunct Prof. Paula Kiuru, Ph.D.

Title of diploma thesis: Synthesis of aerothionin analogs as potential antimycobacterial agents

Key words: antimycobacterial; tuberculosis; synthesis; aerothionin; bromotyrosines

Drugs currently used for the treatment of tuberculosis are the result of studies carried out 50 or 60 years ago. With the constantly growing bacterial resistance to these pharmaceuticals grows also the importance of research for new antimycobacterially active compounds. The marine environment undoubtedly holds an enormous potential for discovering new leads for the development of antitubercular agents. One of these leads is a spirocyclic compound called aerothionin (**1**), which was found to be active against multidrug-resistant strains of *Mycobacterium tuberculosis*, as well as three non-tuberculosis mycobacteria (**Figure 1**). In addition, several spirocyclic structures (not only from marine origin) were discovered to affect on the *M. tuberculosis* in recent years, making this structure segment attractive for antitubercular research.

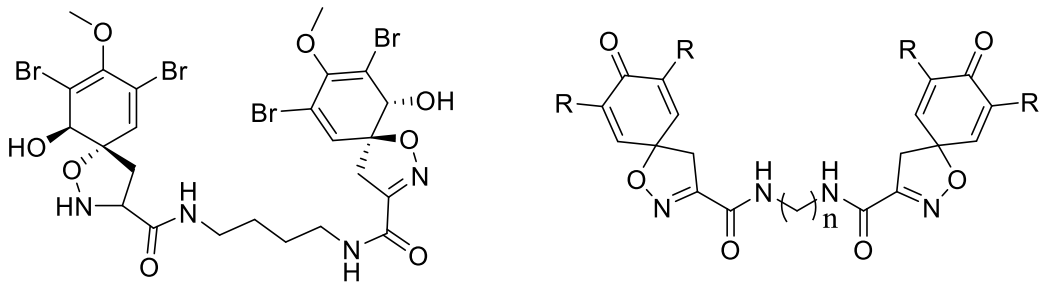

Figure 1: Aerothionin (**1**) and general structure of the products.

Following these promising results, the present thesis project is based on the development of bromotyrosine derivatives similar to aerothionin with the aim to optimize their biological activity as well as their synthesis by removing some of the functional groups. Starting from L-tyrosine, through four step synthesis, 7,9-dibromo-8-oxo-1-oxa-2-azaspiro[4.5]deca-2,6,9-triene-3-carboxylic acid (**MS-4**) and 8-oxo-1-oxa-2-azaspiro[4.5]deca-2,6,9-triene-3-carboxylic acid **(MS-11)** were prepared and subsequently subjected to coupling reactions in order to achieve the desired products.

MS-4 and **MS-11** were obtained without significant complications, however, the amide coupling turned out to be quite problematic. More than ten synthesis approaches were tried for the syntheses of diamides, but only two of them proved to be successful, resulting in three final products (and one intermediate) that differ in the substitution of the aromatic ring. These products were tested for their antimycobacterial activity *in vitro*, using *Mycobacterium marinum* as a test organism. Compound **MS-20** showed the best results, when during first 48 hours performed better than rifampicin control treatment and decreased relative luminiscence under 1 % of the initial value before 24 h, when administered together with rifampicin.

3 ABSTRAKT (SLOVAK)

Univerzita Karlova

Farmaceutická fakulta v Hradci Králové

Katedra farmaceutickej chémie a farmeceutickej analýzy

Riešiteľ: Martina Šimovičová

Vedúci diplomovej práce: doc. PharmDr. Jan Zitko, PhD.; Adjunct Prof. Paula Kiuru, Ph.D

Názov diplomovej práce: Syntéza analógov aerothionínu ako potenciálnych antimykobakteriálnych zlúčenín

Kľúčové slová: antimykobakteriálny, tuberkulóza, syntéza, aerothionín, bromotyrozíny

Liečivá súčasne používané na liečbu tuberkulózy sú výsledkom štúdií uskutočnených pred 50 alebo 60 rokmi. So stále narastajúcim problémom rezistencie baktérií na súčasne používané liečivá rastie i význam výskumu zaoberajúceho sa hľadaním nových antimykobakteriálne účinných látok. Morské prostredie má nepochybne obrovský potenciál pre objav nových vedúcich štruktúr pre vývoj antituberkulotických zlúčenín. Jednou z týchto vedúcich štruktúr je spirocyklická zlúčenina aerothionín (**1**), u ktorej bola zistená aktivita proti multirezistentným kmeňom *Mycobacterium tuberculosis*, spolu s troma netuberkulotickými mykobaktériami (**Obrázok 1**). Navyše, v posledných rokoch sa u viacerých spirocyklických zlúčenín zistilo, že pôsobia na *M. tuberculosis*, čo robí tento štruktúrny segment atraktívny pre antituberkulotický výskum.

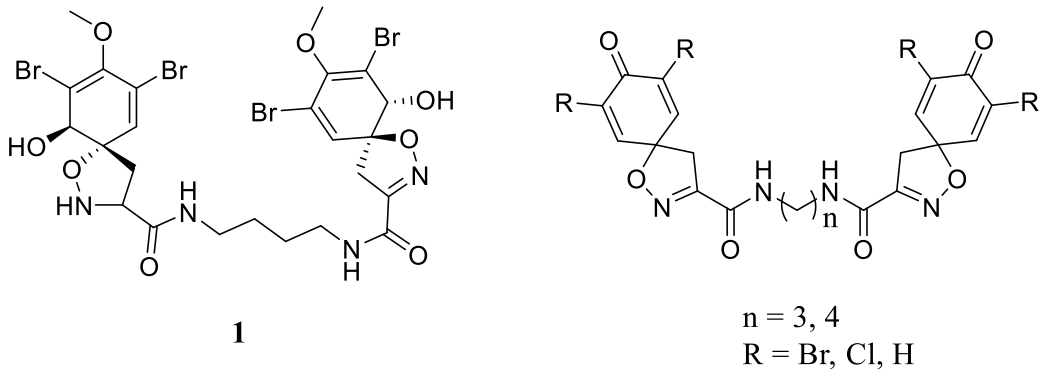

Obrázok 1: Aerothionín (1) a všeobecná štruktúra produktov.

Nadväzujúc na tieto sľubné výsledky, súčasná diplomová práca je založená na tvorbe bromotyrozínových derivátov podobných aerothionínu s cieľom optimalizovať ich biologickú aktivitu a zároveň ich syntézu odstránením niektorých funkčných skupín. Začínajúc od L-tyrozínu, štvorkrokovou syntézou boli pripravené 7,9-dibromo-8-oxo-1-oxa-2-azaspiro[4.5]deka-2,6,9-triene-3-karboxylová kyselina (**MS-4**) a 8-oxo-1-oxa-2-azaspiro[4.5]deka-2,6,9-triene-3-karboxylová kyselina **(MS-11)**, ktoré boli následne podrobené reakciám za vzniku amidovej väzby, aby sme získali želané produkty.

MS-4 and **MS-11** sme dosiahli bez závažnejších komplikácií, avšak tvorba amidovej väzby sa ukázala byť pomerne problematická. Vyskúšali sme viac ako desať syntetických metód, ale iba dve z nich boli úspešné, výsledkom čoho sú tri finálne produkty (a jeden medziprodukt) líšiace sa substitúciou aromatického jadra. Tieto produkty boli testované na svoju antimykobakteriálnu aktivitu *in vitro* s použitím *Mycobacterium marinum* ako testovaného organizmu. Najlepšie výsledky ukázala zlúčenina **MS-20**, ktorá si počas prvých 48 hodín viedla lepšie ako rifampicínová kontrolná vzorka a znížila relatívnu luminiscenciu pod 1 % pôvodnej hodnoty za menej ako 24 h, keď bola podaná spolu s rifampicínom.

4 AIM OF WORK

The fact that marine sponges encompass antibacterially active compounds has been reported as a general phenomenon[1], and it encourages scientists for investigations in the field of antibiotic research, including tuberculosis treatment. Several antimycobacterial substances were discovered in sponges of the order Verongida[2–4], with the most promising compound aerothionin (**1**)[5], effective against several multidrug-resistant Mtb, hinting towards a new mechanism of action.

Based on the consideration that structural simplification of natural products (that are often difficult to obtain or synthesize in high amounts) is a strategy to improve pharmacological profile of these molecules, the aim was to synthesize a library of aerothionin analogs with simplified features. Spiro-sturucture was to be simplified and the chiral hydroxyl moiety removed which will help to understand what structural characteristics are essential for the antitubercular activity and which ones can be omitted to make the future synthesis faster and more feasible. The bromine functional group was to be replaced with chlorine or hydrogen; allowing various combinations using differently substituted starting materials. The prepared analogs were to be subjected to screening for their biological activity.

5 THEORETICAL BACKGROUND

5.1 Introduction

Globally, 7.1 million people with tuberculosis (TB) were reported to have been newly diagnosed in 2019. Despite substantial efforts in the last decade, the success in controlling this disease is very low with the rate of TB cases declining just 1.5 % per year. TB tops among the "neglected" diseases of the developing world. About a quarter of the world's population is infected with *Mycobacterium tuberculosis* (Mtb).[6] (**Figure 2**)

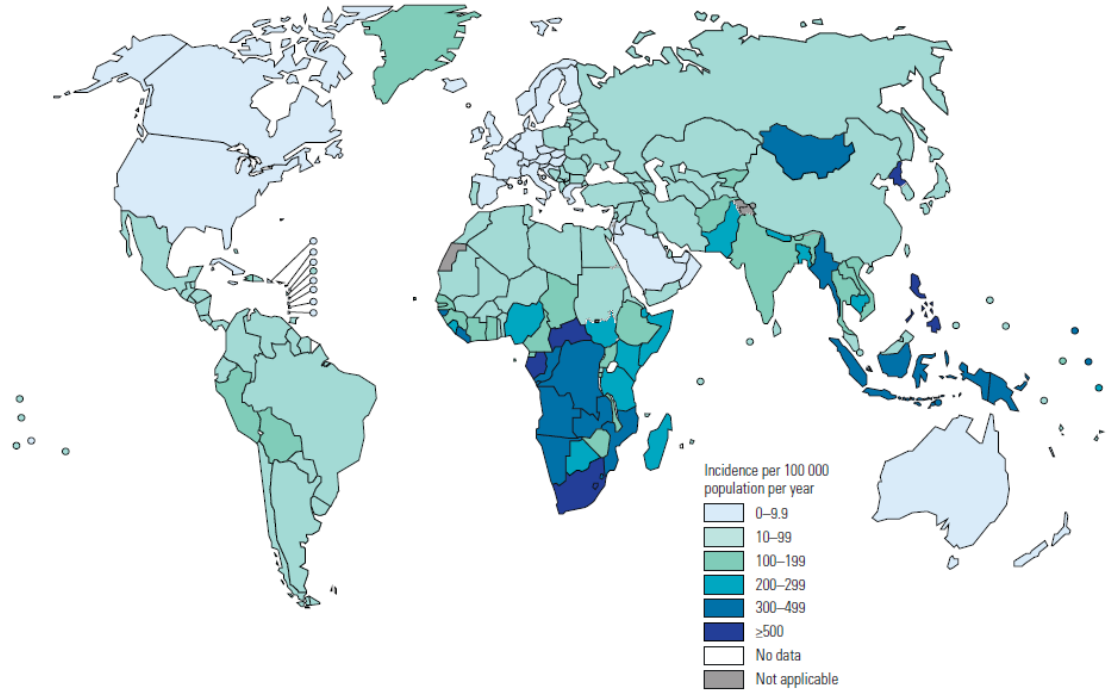

Figure 2: Estimated tuberculosis incidence rates in 2019. Taken from WHO: Global tuberculosis report 2020.[6]

5.2 Mycobacteria

Mycobacteria are aerobic, acid-fast, nonmotile, non-encapsulated bacteria belonging to the order *Actinomycetales* and family *Mycobacteriaceae*. The main distinguishing characteristic is a thick hydrophobic cell wall, which is rich in mycolic acids/mycolates.[2] This coating makes the cell impermeable to Gram staining[7] and is the main reason for the hardiness of this genus, allowing the mycobacteria to withstand long exposure to acids, alkalis, detergents, oxidative bursts, lysis by complement, dehydration, and many antibiotics.[8] Mycobacteria can be divided into *Mycobacterium tuberculosis* complex, which can cause tuberculosis (e.g. *M. tuberculosis*, *M. bovis*, *M.*

africanum); *M. leprae*, which causes leprosy; and nontuberculosis mycobacteria (e.g. *M. avium, M. intracellulare, M. marinum, M. kansasii)*, which can cause pulmonary disease resembling tuberculosis, skin disease, lymphadenitis, or disseminated disease.[8]

Mycobacterium marinum is a waterborne mycobacterium that causes tuberculosis-like illness in fish and frogs. It can cause a granulomatous skin disease in humans, when injured skin gets into contact with contaminated water. For this reason, it most commonly infects aquarium keepers. Infection is usually localised only in skin and soft tissues, but ocassionally can take disseminated form in immunocompromised patients.[9,10]

M. marinum is closely related to Mtb with their 99.3 % 16SrRNA sequence homology and shares common characteristics, like ability to survive inside macrophages or giving a positive tuberculin skin test. However, unlike Mtb, *M. marinum* grows rapidly at 32°C, when the replication time in the laboratory is 4 hours (for Mtb it is 24 hours at 37°C in the laboratory). At the infection site (37°C), their growth is similar, with 24 hours for one generation.[9]

For these reasons (a relatively fast growth, minimal risk for laboratory personnel and similar pathogenic mechanisms to human tuberculosis), *M. marinum* has been used as mycobacterial infection model.[10,11] Pouty et al. described using zebrafish (*Danio rerio*) for both acute and chronic infection studies with advantages such as easy maintenance, quick breeding, tractable genetics and highly similar immune system including macrophages, B- and T-cells.[11]

5.3 Tuberculosis

Tuberculosis is an infectious disease caused by *M. tuberculosis*, which is transferred by aerosols and prevailingly affects the lungs, but can damage any tissue. Mtb can be found only in humans, although the related pathogenic mycobacteria, *M. bovis*, causes disease in cattle. Before milk pasteurization, *M. bovis* was the cause of scrofula, TB of the lymph nodes. Mtb is able to persist in people for a long time, with only a certain percentage of people developing clinical disease with lung damage.[12] (**Figure 3**)

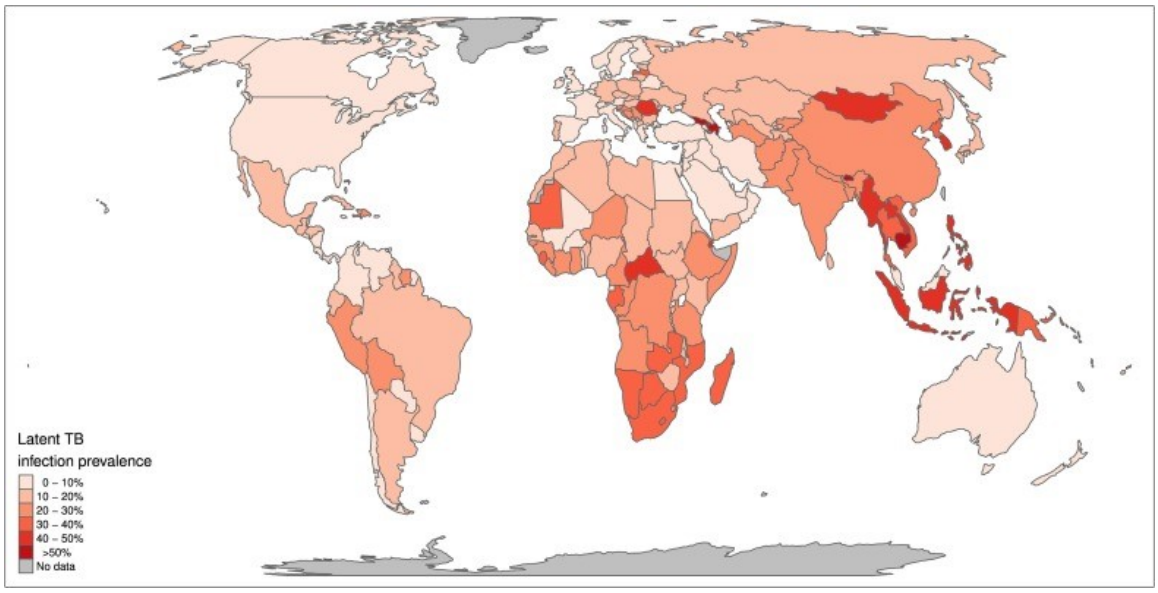

Figure 3: Median estimated population prevalence of latent Mtb infection by country, 2014. Taken from Houben et al.[13]

TB is transmitted from person to person through aerosol droplets from the respiratory tract of people with active disease. Individuals with pulmonary or laryngeal tuberculosis produce droplets while sneezing, coughing, or speaking. Inhaled infectious droplets stay in the lung alveoli and bacilli are there taken up by macrophages.[12]

In most healthy people, infection with Mtb does not cause any symptoms, since the person's immune system reacts to kill or shutter the bacteria (formation of granulomas, which limits further replication and spread of the organism). A relatively small proportion (5–10 %) of people infected with Mtb worldwide will develop tuberculosis during their lifetime. However, the probability is significantly higher for people with HIV/AIDS co-infection, and among people affected by risk factors such as malnutrition, diabetes mellitus, immunosuppressive therapy, smoking and alcoholism.[7,12,14] (**Figure 4**)

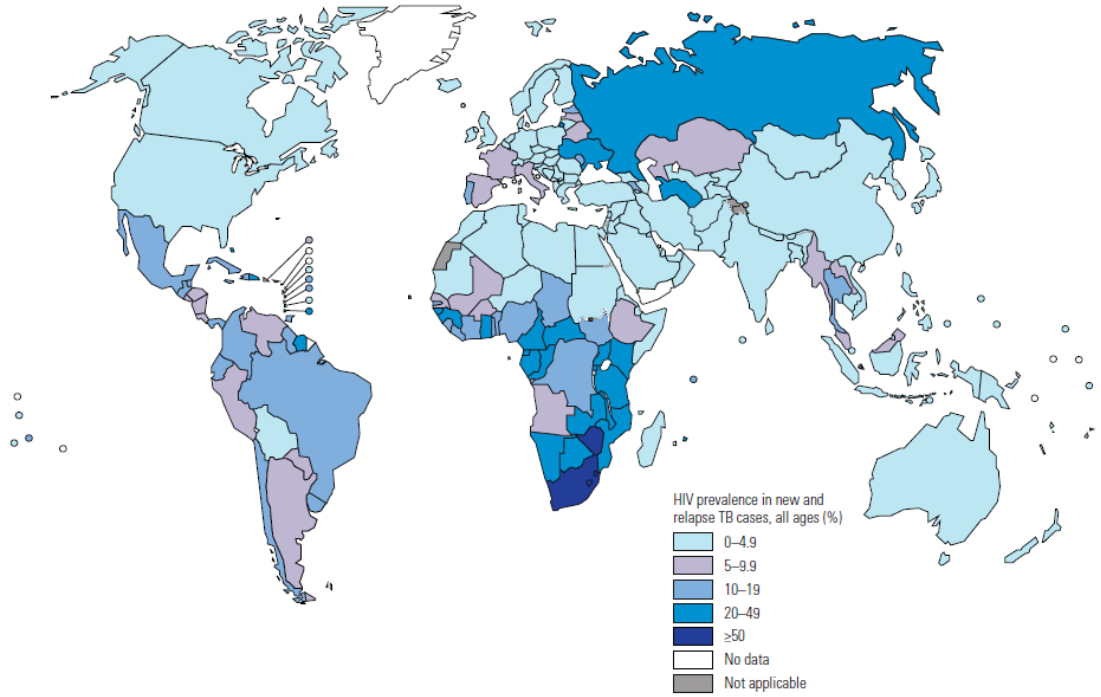

Figure 4: Estimated HIV prevalence in new and relapse TB cases, 2019. Taken from WHO: Global tuberculosis report 2020.[6]

The symptoms of active TB of the lung are coughing, sometimes with blood in sputum; fever, chest pains, weakness, weight loss, and night sweats. Extrapulmonary tuberculosis makes up 10–30 % of disease and is more common among women and children and in HIV/AIDS infected people.[6] Latent TB has significant impact on the tuberculosis population dynamics and epidemiology, since it serves as a huge reservoir of potential disease and further transmission.

5.3.1 TB and COVID-19

The coronavirus pandemic (COVID-19) has affected also tuberculosis. There is already evidence from several high TB burden countries of large reductions in the number of people with TB being detected in 2020.[6] The possible reasons are that people with mild symptoms did not seek medical care to lessen crowding in health facilities, restrictions in movement made it more difficult for people to travel to healthcare centres, reductions in the number of health facilities offering TB diagnostic and treatment services, reallocation of personnel, finances and diagnostic machines to COVID-19, and loss of wages[12] that increases poverty and undernutrition.

There is still little information about whether tuberculosis acts as a risk factor for progression of COVID-19. Meta-analysis done by Gao et al.[15] showed that while people

with tuberculosis were not more susceptible to get COVID-19, pre-existing tuberculosis caused a 2.1-fold higher chance of developing severe COVID-19 illness. However, because of a small amount of reports, more studies are needed to better understand the effect of tuberculosis on COVID-19 prognosis.

5.3.2 Diagnosis

Diagnosis in low- and middle-income countries is made primarily by sputum smear microscopy and chest radiology, however, the microscopy is capable of detecting only 50–60 percent of all cases (smear-positive).[12] More sensitive methods of diagnosing TB and detecting resistance to drugs are more expensive, including rapid molecular tests (first approved by WHO in 2010) and culture-based methods. Among the new diagnostic options, the Xpert MTB/RIF test has received the most attention for it's fast (less than 2 hours) and sensitive detection of TB and rifampicin resistance. WHO recommended using the device for initial diagnosis in patients suspected of having multidrug-resistant TB (MDR-TB) or HIV/AIDS-associated TB disease.[16] Exposure to TB can be detected by tuberculin skin test (TST), which indicates cell-mediated immunity to TB and is used as standard method for diagnosis of latent TB infections.[17] Tuberculosis is particularly difficult to diagnose in children, where it is often overlooked.[6]

5.3.3 Prevention

The strategies for preventing TB consist of vaccination, infection control, and chemoprophylaxis or isoniazid preventive therapy (IPT).[6] The only vaccine in the world is bacille Calmette-Guérin (BCG) vaccine, which is widely used and is effective at preventing tuberculous meningitis and disseminated (miliary) TB in children. There is no vaccine that could protect adults from developing TB, however it is recommended for people with HIV, living in the household with people with confirmed TB or risk groups (e.g. people receiving dialysis) to take chemoprophylaxis, most commonly IPT, for a latent infection.[18]

5.3.4 Treatment

The current standard WHO-approved regimen is rifampicin (**2**), isoniazid (**3**), ethambutol (**4**) and pyrazinamide (**5**) (**Figure 5**) for two months (intensive phase) followed by isoniazid and rifampicin (with or without ethambutol in areas with high resistance) for four months (continuation phase).[19]

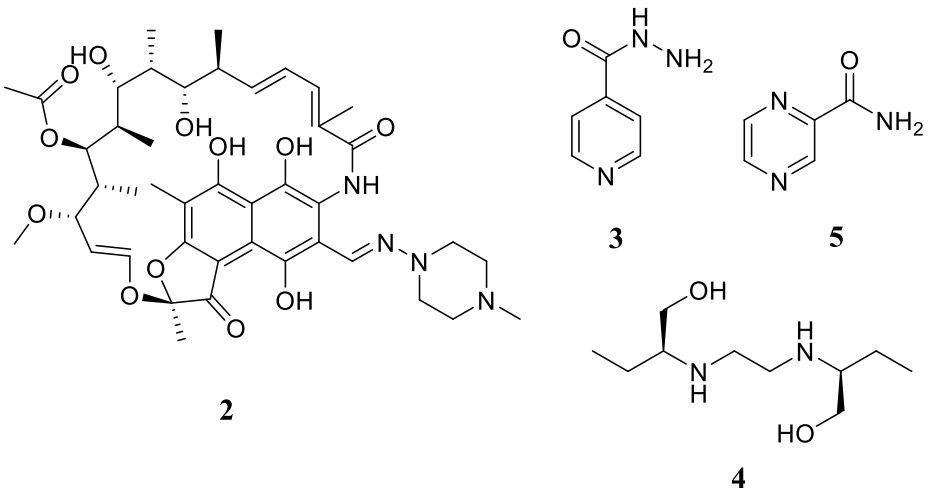

Figure 5: Structures of first-line antimycobacterial drugs: rifampicin (**2**), isoniazid (**3**), ethambutol (**4**) and pyrazinamide (**5**).

Treatment for people with MDR TB (resistance to isoniazid and rifampicin, multidrug-resistant tuberculosis) and XDR TB (extensively drug-resistant tuberculosis, resistance to isoniazid, rifampicin, at least one fluoroquinolone and one injectable antitubercular antibiotic) is longer, and requires drugs that are less effective, more expensive and more toxic. Second line agents include streptomycin (**6**), amikacin, kanamycin, capreomycin, fluoroquinolones, ethionamide (**7**), and *p*-aminosalicylic acid (**8**).[20] (**Figure 6**)

This long drug regimen is challenging for both patients and health care systems, especially in low-income countries, where the financial resources and adherence are not optimal and is a main reason for mycobacterial resistance. Hence, shortening the duration of treatment for individuals with either drug-sensitive or drug-resistant tuberculosis is a global research priority.

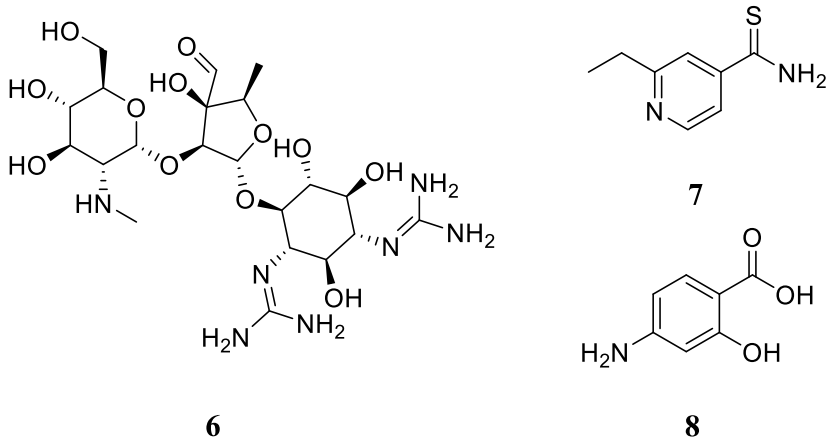

Figure 6: Structures of streptomycin (**6**), ethionamide (**7**) and *p*-aminosalicylic acid (**8**).

Currently, new drugs are being studied for the treatment of tuberculosis, including repurposing of existing drugs; e.g. rifamycins (rifabutin and rifapentine), nitroimidazoles, diarylquinolines, oxazolidinediones, and ethylenediamines.[12]

Between novel chemical entities developed for anti-TB therapy belong bedaquiline (**9**), delamanid (**10**) or pretomanid (**11**).[21] (**Figure 7**) New drug combinations including these pharmaceuticals, which are thought to act on new molecular targets, are also being introduced.[12]

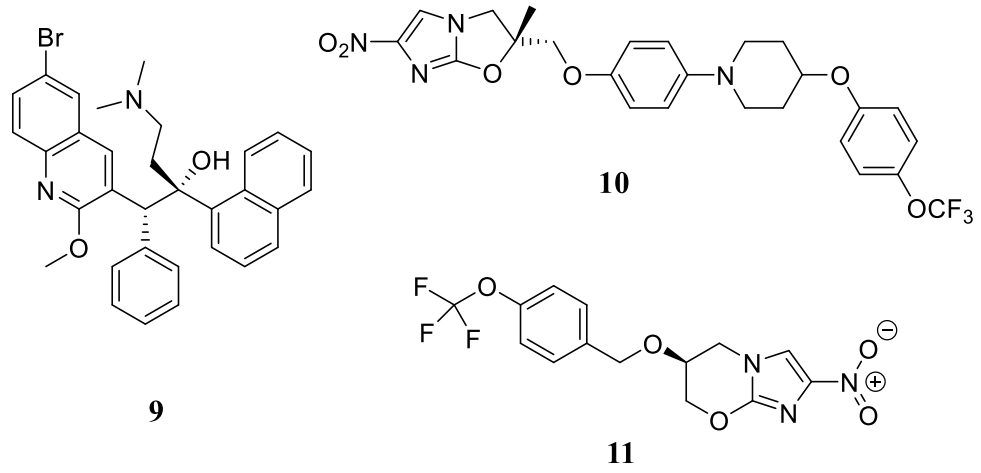

Figure 7: Structures of bedaquiline (**9**), delamanid (**10**) and pretomanid (**11**).

5.3.5 Resistance

Antimicrobial resistance occurs when microbes (bacteria, viruses, fungi) change and no longer respond to medicines that were effective before. This threatens our ability to treat common infectious diseases like pneumonia, salmonellosis, gonorrhoea, or tuberculosis.[22]

The resistance crisis has been attributed to the overuse and misuse of drugs, as well as a deficit of new medicine development because of reduced economic stimulus and challenging regulatory requirements. Incorrectly prescribed antibiotics have questionable therapeutic benefit while the subinhibitory concentrations support gene expression and mutagenesis. Antibiotics are also widely used as growth supplements in livestock. The antibiotics used in livestock are then ingested by humans while eating.[23]

The emergence of highly drug-resistant tuberculosis, including MDR TB and XDR TB, has proved a serious obstacle for effective control of the disease.[12] A better

understanding of drug tolerance in Mtb is important as it may allow the development of new treatment-shortening strategies that prevent formation of drug tolerance.

Whether the mycobacteria survive or not strongly depends on their ability to quickly respond to stress.[24] The published literature[24,25] shows that several biological pathways are involved in the formation of drug-tolerant state. The main mechanisms are:

a) metabolic shutdown – most antibiotics attack metabolically active Mtb[25]; slowing metabolism and growth rate through downregulation of genes involved in aerobic respiration, ATP synthesis, lipid metabolism and protein synthesis[24] is therefore very effective;
b) metabolic shifting – rerouting metabolite fluxes to preserve homeostasis when specific pathways are attacked by medicines[25]; typically shifting from growth-promoting Krebs cycle to carbon storage in fatty acids via synthesis of triacylglyceroles under stress conditions, including drug pressure (**Figure 8**);

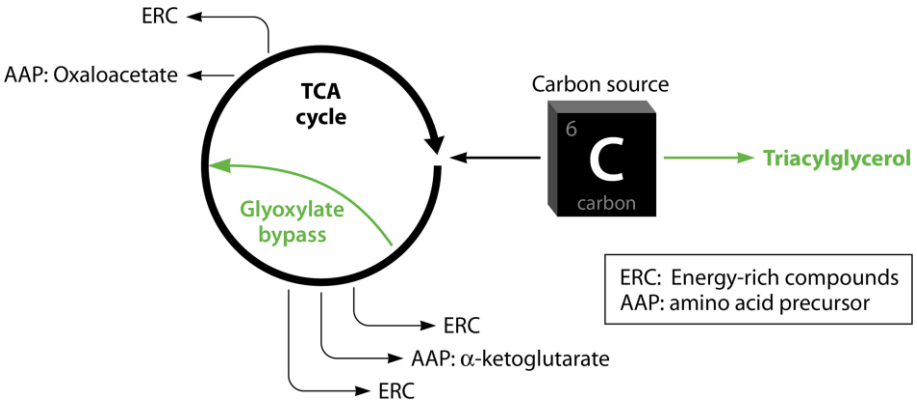

Figure 8: Methabolic shifting of carbon fluxes away from the TCA cycle. Taken from Goossens et al.[25]

c) cell wall thickening – mycobacterial cell wall is naturally a very tough barrier that medicines have to overcome; more thinckening slows down the uptake of lipophilic drugs while porins may not be able to bridge the increased cell width and thus hydrophilic drugs can not get through[26]; interesting is that thickening occurs only under microaerobic or anaerobic conditions and is connected with metabolic shift to anaerobic processes[24] mentioned in b) (**Figure 9**);

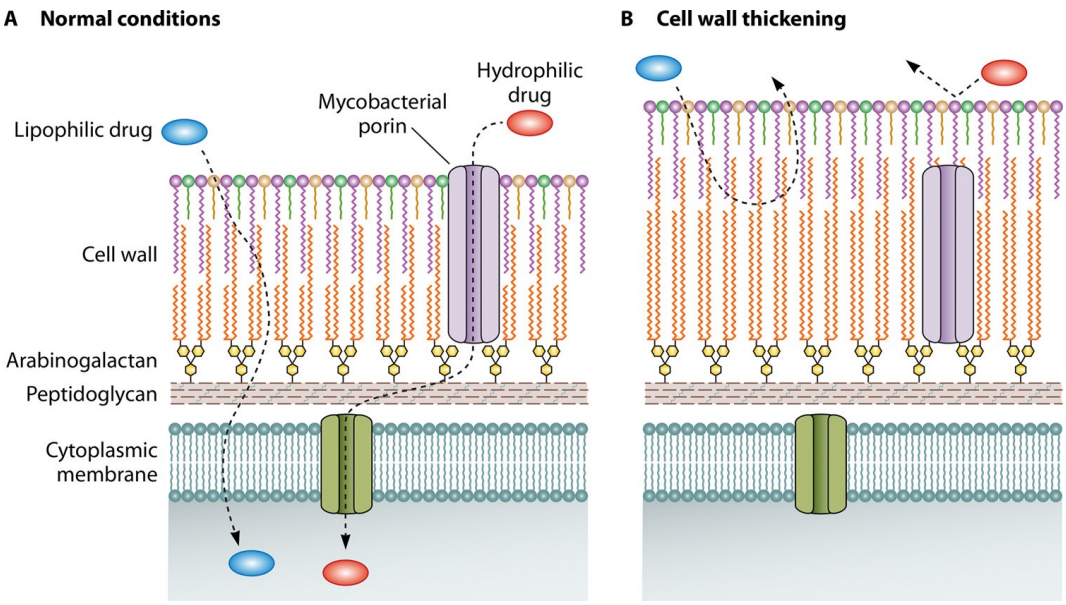

Figure 9: Cell wall thickening. Taken from Goossens et al.[25]

d) upregulation of efflux pumps – several efflux pumps have been found to be upregulated under antibiotic stress, increasing the clearance of antibiotics out of the cell;[25] this process can be non-specific, when upregulation of efflux activity induced by one drug can cause reduced sensitivity to other antimicrobials;[27]

e) genetic adaptations contributing tolerance – specific genetic variants can increase the probability of Mtb to become resistant, e.g. "high-persisting" (*hip*) mutants that often manifest as reduced lipid metabolism, similar to metabolic shifts from Krebs cycle to lipid synthesis.[28]

What´s more, several bacterial populations with different growth dynamics were found in a sputum of a single patient, which suggests that mycobacterial populations are heterogenous[25], which contributes to the variability in responses to the treatment.

5.3.6 In vitro antimicrobial testing methods of the new compounds

When new compounds, either synthesized in a laboratory or isolated from nature, are suspected for having antimycobacterial properties, there are several antimicrobial susceptibility testing methods available. Disk-diffusion and broth or agar dilution methods belong to the most known and basic methods, however, to better understand the antimicrobial effect of a molecule (bactericidal or bacteriostatic, time-dependent or concentration-dependent), time-kill test or flow cytofluorimetric methods are recommended.[29]

5.3.6.1 Agar diffusion

In this procedure, filter paper disks containing test compounds are placed on the agar surface previously inoculated with the test organism.[29] The tested molecules diffuse into the agar and inhibit growth of the microorganism. The agar plate is then incubated and after a set period of time (depending on the microbe), diameters of the growth inhibition zones are measured.[30] While this method is very simple and does not require special equipment[31], it has several disadvantages. Agar diffusion method gives us information about whether the microorganism is susceptible or resistant to the tested compound, but the minimum inhibitory concentration (MIC) cannot be determined, since it is impossible to quantify the amount of the compound diffused into the agar.[29] Moreover, non-polar compounds diffuse significantly slower in the aqueous agar medium and therefore seem to be less effective than more polar molecules.[30] Since Mtb possesses a thick hydrophobic cell wall, not being able to compare less-polar molecules (that are often more active) to for example standard antibiotics becomes a reason to avoid diffusion assays.[32]

5.3.6.2 Antimicrobial gradient method

This method combines diffusion and dilution methods in order to determine the MIC value. A strip impregnated with an increasing concentration gradient of the (potentially) antimicrobial compound is laid on the surface of the agar plate inoculated with the microorganism. Since the concentration of antimicrobial agent ranges from one end of the strip to other, we are able to determine MIC easily and this method shows good correlation between MIC values obtained by dilution methods. The main problem represents the cost of the strip, making the method less atractive when large numbers of compounds are tested.[29]

5.3.6.3 Dilution methods

The main advantage of dilution methods is the possibility to determine the MIC value, since the concentration of the tested antimicrobial agent in broth medium (macrodilution or microdilution) or agar (agar dilution) is known.[29] Two-fold dilutions of the tested compound in the liquid growth medium are prepared and distributed in tubes (macrodilution) or in microtitration plate (microdilution).[29,32] After that, a microbial inoculum prepared in the same liquid medium is added and left for incubation. Microdilution is usually preferred because of the considerably lower amount of reagents and space needed and, what's more, when combining the method with

spectrophotometric or fluorimetric detectors for plate reading, enormous output can be achieved.[32] The problem appears with the tendency of mycobacteria to clump, since the microbial growth is usually quantified by turbidity in liquid medium.[30,32] This problem can be solved using dyes, e.g. Alamar Blue, 2,3,5-triphenyltetrazolium chloride or 3-(4,5-dimethylthiazol-2-yl)-2,5-diphenyltetrazolium bromide, with which the growth or inhibition can be measured colorimetrically or fluorometrically.[29,32]

Agar dilution consists of incorporation of the tested molecule (usually in two-fold concentrations) into the agar medium and subsequent inoculation of the microbe. Then the MIC is the lowest concentration that completely inhibited the microbial growth. Agar dilution is often used when the tested compound interferes with the detection with its coloring or if several microbial isolates are tested against a single substance.[29]

5.3.6.4 Time-kill test

To distinguish between time-dependent and concentration-dependent antimicrobial effect, time-kill test is the method of choice.[29] In this method, three tubes with a bacterial suspension are used: the first and second tube contains the tested molecule at 0.25-fold and 1-fold MIC concentrations, respecvtively; the third one is for comparison. While incubating, at selected time intervals the amount of the dead cells is measured and calculated as a percentage compared to the growth control in the third tube using agar plate count method. The effect of the tested compound is considered bactericidal when the lethality percentage after six hours reaches 90 %.[29]

5.3.6.5 Radiometric assays

These radiometric assay systems are based on measuring the uptake of radioactively marked compounds into the mycobacterial cells. A BACTEC radiometric testing method measures radioactive carbon dioxide produced by the metabolism of radiolabelled palmitic acid.[32] Another technique uses radioactive uracil and a strain of *Mycobacterium aurum*, which grows faster than Mtb, does not have such an infectious nature (it's a saphrophyte) and can be used for prediction of the Mtb inhibition.[33] This screening method allows to test multiple thousand samples per day[33]; however, its usage is costly and brings the problem of radioisotope disposal (as well as all other radiometric methods).[32]

5.3.6.6 Bioluminiscence assays

One of the possibilities is to measure adenosine triphosphate (ATP) produced by Mycobacteria. As ATP serves as an energy storage for the cells, it is present in all living cells and can be used to quantify the viability of mycobacterial population. In the presence of ATP, D-luciferin is converted by luciferase to oxyluciferin, that generates light. There is a linear correlation between the number of living mycobacterial cells and the luminiscence emitted.[29]

Andreu et al.[34] described a bioluminiscence method that does not need external addition of substrate for the production of light. They used mycobacteria containing bacterial *lux* operon and thus generating luminiscence on their own. The advantage is that this method can be used for screening also inside macrophages, which was before possible only by CFU (colony forming units) plating that is time consuming and required killing the macrophages. However, this measurement is non-destructive and therefore allows to collect data at various timepoints for discovering the inhibition kinetics.

The fast results are the main advantage of bioluminiscence screening assays - 3-6 days compared to conventional dilution methods (3-4 weeks) with proportionate results.[29,34]

5.3.6.7 Flow cytometry

Flow cytometer measures scattered lights and fluorescence emissions from thousands of cells that pass one by one through laser beams.[35] The cells are dyed with fluorescent staining, such as fluorescein diacetate (administered as a nonfluorescent diacetylester, that becomes fluorescent when hydrolysed by cytoplasmatic esterases), SYTO 16 (a nucleic acid dye that penetrates only into cells with damaged membrane) or propidium iodide.[29,32] Thanks to this staining viable and damaged/dead cells can be distinguished. Time needed to obtain the results ranges from two to six hours[29], which makes flow cytometry a very promising technique for antimycobacterial susceptibility testing. However, high cost of flow cytometry equipment limits its application in various laboratories.[32]

5.4 Spirocyclic compounds with antitubercular activity

In the last ten years, compounds with spirocyclic segment in the structure have become interesting for scientists looking for new antitubercular agents. In 2014, GlaxoSmithKline (GSK) published structures of 177 small molecules and their anti-TB activities that were chosen as possible leads for future research according to the tests on

the Mycobacteria growth inhibition, cytotoxicity and physical properties.[36] Seven of them contained spirocycle core, thus they were named Spiros by GSK. The Spiros are believed to affect on membrane transport protein (Mycobacterial membrane protein large 3, MmpL3), which was recently identified as essential for viability of Mtb.[37,38]

Guardia et al.[37] followed up on this research with the aim to synthesize effective analogs with improved profile, since the original compounds displayed low microsomal stability. The result was compound **12 (Figure 10)**, which showed high potency in murine infection model and good pharmacokinetic properties. However, further development of this compound as an antitubercular drug were halted by high hepatotoxicity risk.[37]

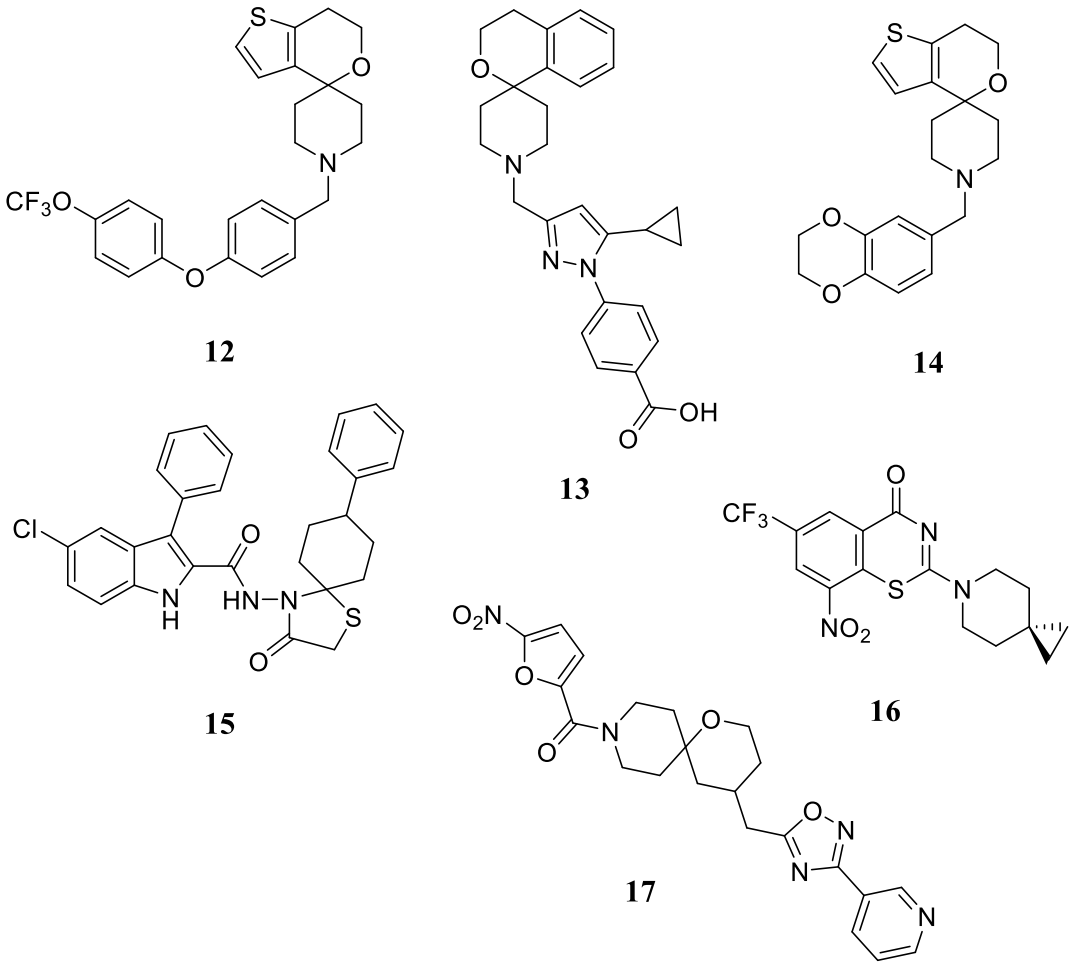

Figure 10: Structures of anti-TB compounds with spirocyclic scaffold.

Ray et al.[39] described a series of zwitterionic molecules, from which **13** was identified as a promising lead with good efficacy in vitro against Mtb strains resistant to isoniazid or rifampicin and better selectivity towards Mtb compared to **12** (reduced

hepatotoxicity). Unfortunately, **13** failed at *in vivo* models, probably because of low *in vivo* exposure.[39]

Badiola et al.[40] also followed the results published by GSK and synthesised novel Spiro analogs. Although prepared compounds exhibited excellent inhibitory activity against Mtb, this came together with toxicity against human monocytic cell lines. Compounds that displayed lower toxicity were also less active than the original GSK structure (**14**).[40]

A series of indole-based spirocyclic thiazolidinones were evaluated for their antimicrobial activity by Cihan-Ustundag et al. Compound **15** showed significant antitubercular activity at concentration tenfold lower than the concentration cytotoxic for mammalian cell lines.[41] Cihan-Ustundag defined indole-spirothiazolidinone segment as a promising scaffold for the antimycobacterial drugs.[42]

Spirocyclic and bicyclic 8-nitrobenzothiazinones were prepared by Zhang et al.[43] in order to improve low water solubility (and thus probable bad bioavailability) of previously known compounds[44] with good activity against Mtb. Molecule **16** with spirocyclic fragment turned out to be the most potent analogue with MIC 16 nM. However, **16** was rapidly metabolized in mouse liver microsomes, so researchers preferred a different bicyclic compound instead.[43]

Another compound efficient against Mtb (**17**) was developed by attaching spirocyclic piperidines to 5-nitrofuryl moiety. By this, Krasavin et al. managed to reduce the non-specific toxicity of nitrofurans and obtain a selectively antimycobacterial compound active also against multidrug-resistant strains.[45]

From the structures mentioned above follows that spirocyclic compounds may be considered as promising pharmacophores for antimycobacterial drug discovery and further structural modifications can lead to new derivatives with even better pharmaceutical potential.

5.5 Antimycobacterial compounds of marine origin

Marine organisms play an important role in drug research as an inexhaustible source of bioactive compounds with unique chemical features and a wide spectrum of biological activities. Since most marine invertebrates, such as sponges, corals and algae are sessile and soft bodied organisms that lack morphological defense mechanisms[46], their survival

depends on the production of secondary metabolites with antimicrobial or repellent effects.[47] The accumulated defensive chemicals protect these organisms from a plenty of stress factors, e.g. predation, overgrowth of smearing organisms, or invasion by pathogenic microorganisms.[48] Secondary metabolites isolated from marine organisms have proven to be an rich source of molecules with pharmacological activities potentially beneficial to human health[47], including the treatment of tuberculosis.

What's more, diversity of natural compounds due to adaptation to a variety of environmental conditions leads to the occurrence of molecules with multiple activities against multiple targets, which might be a solution to the problem with drug resistance, since several genetic mutations would be required.[21,46]

Several substances with antimycobacterial activity were isolated from marine sponges and fungi in the past years.[49] Heteronemin, isolated from *Heteronema erecta*, showed activity against Mtb H37Rv with MIC of 6.25 μg/mL, which started further research of scalarane-type sesterterpenes.[46] This lead to the discovery of a variety of active substances, e.g. 12-deacetoxyscalarin-19-acetate or 12-oxoheteronemin (**18**, **Figure 11**). However, 12-oxoheteronemin displayed strong cytotoxicity[46], which excluded the compound from potential medicinal use.

Kumar and colleagues[50] discovered that a new diarylpyrrole alkaloid denigrin C (**19**) isolated from the extract of the Indian marine sponge *Dendrilla nigra* showed strong activity against Mtb H37Rv with a mechanism of action that yet has to be discovered. Callyaerins A and B, isolated by Daletos and colleagues[51] from the Indonesian sponge *Callyspongia aerizusa* exhibited potent antibacterial activity against Mtb with no toxicity against cancer cell lines. Diterpene alkaloids from sponges *Myrmekioderma styx, Cymbastela hooperi* and *Svenzea flava* also showed considerable activity, including (-)-8,15-diisocyano-11(20)-amphilectene (**20**), which was used as a scaffold for the synthesis of another potential antiinfective agents.[46] Pseudopteroxazole (**21**) and seco-pseudopteroxazole, new benzoxazole diterpene alkaloids from the West Indian gorgonian *Pseudopterogorgia elisabethae*, induced growth inhibition for Mtb H37Rv (97 % and 66 %, respectively) at a concentration of 12.5 mg/mL without significant cytotoxicity.[2]

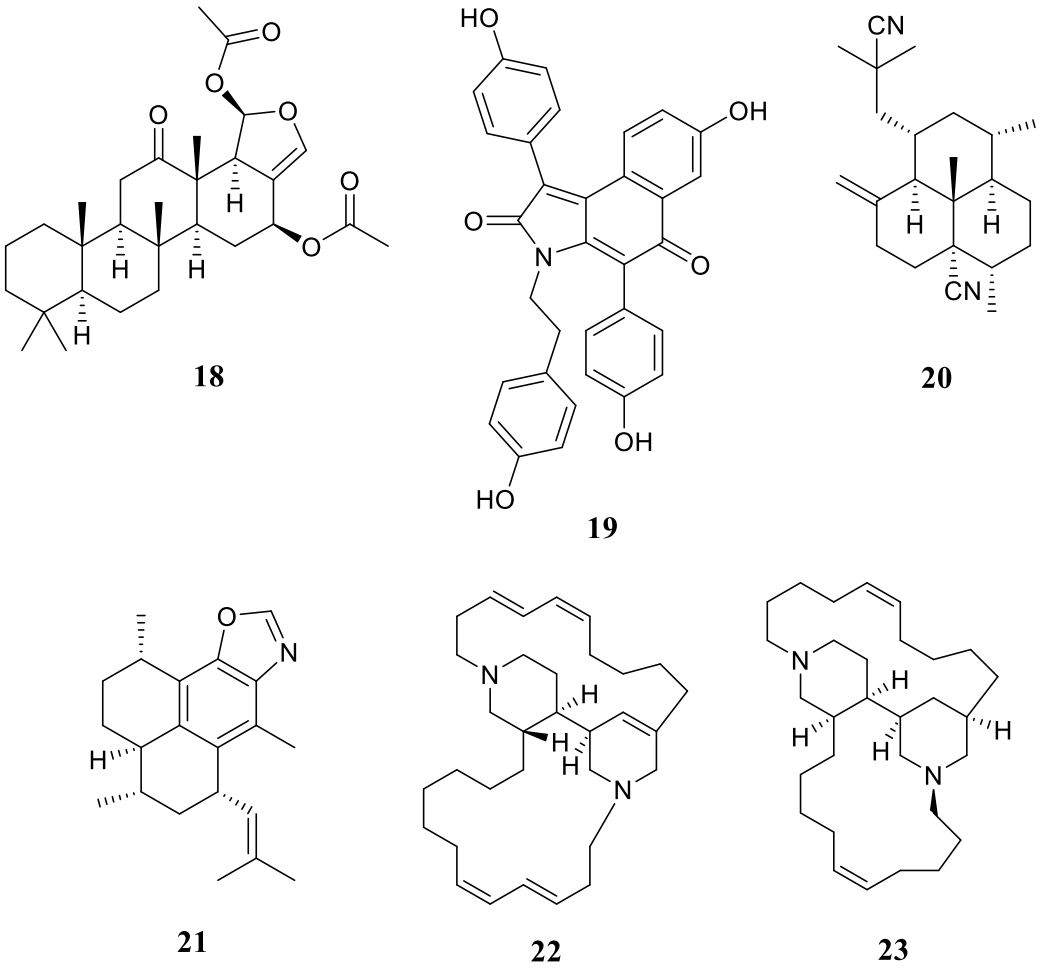

Figure 11: Structures of 12-oxoheteronemin (**18**), denigrin C (**19**), (-)-8,15-diisocyano-11(20)-amphilectene (**20**), pseudopteroxazole (**21**), halicylamine A (**22**) and neopetrosiamine A (**23**)

Activity of halicylamine A (**22**) against Mtb H37Rv, together with activity against *M. avium, M. intracellulare, M. aurum* and *M. kansasii* was revealed by Arai et al.[52] Notably, the MIC values were the same during hypoxic and aerobic assays. The fact that commonly used medicines, e.g. isoniazid considerably lose their efficacy in hypoxic conditions[25,52] makes this discovery very intriguing.

Neopetrosiamine A (**23**) from the marine sponge *Neopetrosia proxima*, was subjected to biological assays against the pathogenic strain of Mtb and several cancer cell lines. The measured inhibitory concentrations showed activity against Mtb as well as melanoma cancer, leukemia and breast cancer with no significant cytotoxicity against Vero cells, which suggests that neopetrosiamine A is not toxic towards physiological human cells.[53]

Lin and colleagues[54] isolated and characterised oxazinin A (**24, Figure 12**) from marine fungus *Lissoclinum patella*, and discovered anti-TB activity of this molecule

at IC_{50} 2.9 μM. The compound underwent also cytotoxicity tests and exhibited only modest activity against human transient receptor potential channels.[54]

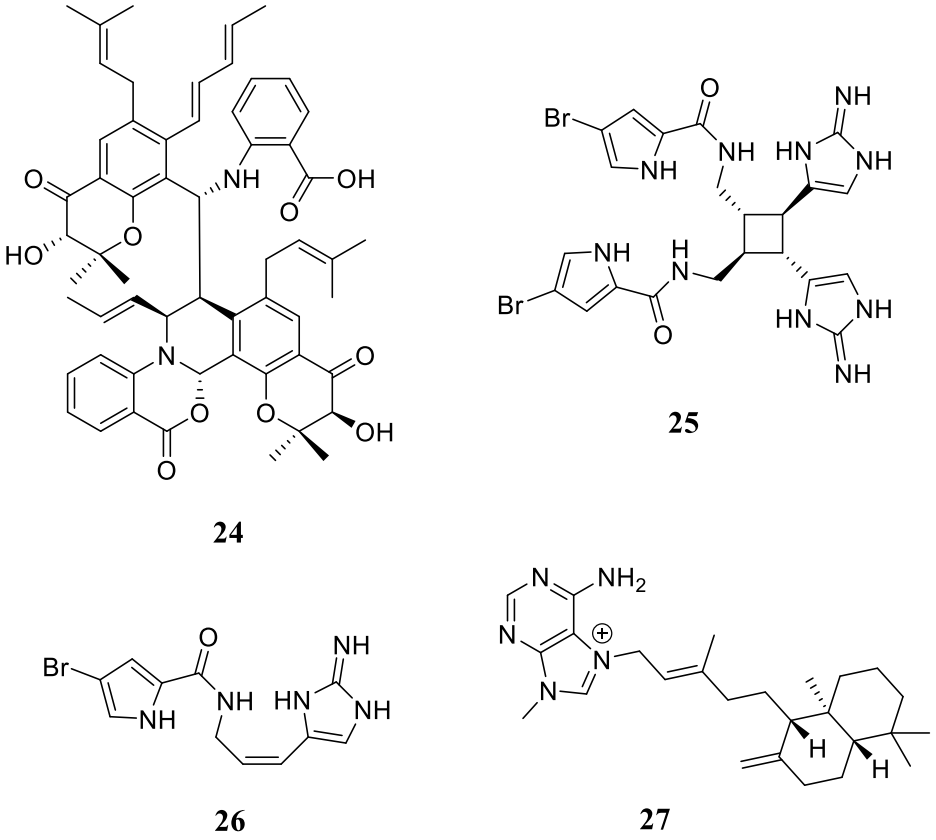

Figure 12: Structures of oxazinin A (**24**), sceptrin (**25**), hymenidin (**26**), agelasine D (**27**).

Pyrrole-2-aminoimidazole alkaloids, which can be found in species Stylissa, Phakellia, Axinella or Hymeniacedon, received a lot of attention for their wide biological activities, including Mtb inhibition.[46] One of the examples is sceptrin (**25**), which inhibited 35 % of Mtb growth at concentration 12.5 μg/mL.[55] Interesting is that the sceptrin's monomer hymenidin (**26**) turned out to be more potent, suggesting that dimerisation is not significant for the activity of these metabolites.[56] In addition, sceptrin showed no cytotoxicity and can be synthetised in multigram quantities, which makes these alkaloids attractive targets for future research.[46]

Agelasines, alkaloids from the genus *Agelas* were rediscovered by Arai and colleagues[57] as anti dormant-mycobacterial substances, effective against both active growing and dormant states of Mtb. Among them, agelasine D (**27**) showed the most potent antimycobacterial activity.[57]

These examples illustrate the importance of examining secondary metabolites derived from the sea, as a possible source of new unexplored antimycobacterial leads.

5.5.1 Bromotyrosines

During this research, we turned our attention to the sponges of the order *Verongida*. For this order is typical production of brominated secondary metabolites that are biogenetically related to tyrosine.[58] These alkaloids raised interests of researchers for more than 50 years for their wide range of biological activities. They were reported to have antibiotic, antiviral, Na+/K+ inhibition, ATPase inhibition, histidine-H_3 antagonist, antifungal, calcium channel regulator and cytotoxic activities.[1]

The bromotyrosine derivatives can be divided into six groups:

1) simple bromotyrosine derivatives
2) spirocyclohexadienylisoxazolines (aerothionin)
3) spirooxepinisoxazolines
4) oximes
5) bastadins
6) other structural types (e.g. geodiamolides, polycitones)

Aerothionin, which belongs to the alkaloids of the *Aplysina* defense cascade, was first isolated by Fattourusso et al.[59] from *Aplysina aerophoba* and *Verongia thiona*. However, later it was also found in other *Aplysina* species, e.g. *A. cauliformis, A. insularis* and *A. gerardogreeni* and several non-*Aplysina* species from order *Verongida* like *Hymeniacidion sanguinea* or *Suberea mollis*. For this reason it is considered one of the chemotaxonomic markers of the *Verongida* sponges, even though some scientists speculate wheteher aerothionin is a product of the sponge itself or from it's bacterial symbionts.[48]

Kernan et al.[60] studied aerothionin for it's activity against *Staphylococcus aureus*, *Bacillus subtilis* and *Candida albicans*. It inhibited the growth of the bacteria at 50 µg/disk. Aerothionin showed activity against *Klebsiella pneumoniae*[58] and inhibited the formation of hyphae in *Streptomyces 85E*[61]. It´s 11-oxosubstituted derivative inhibited *Escherichia coli*, *S. aureus* and *Pseudomonas aeruginosa* in a study by Acosta et al.[62] And finally, Encarnación and colleagues[5] discovered the activity against virulent Mtb strain H37Rv at minimum inhibitory concentration (MIC) 12.5 mg/mL. What's more, at this MIC value, aerothionin was active also against four monoresistant Mtb

strains (isoniazid, rifampicin, ethambutol and streptomycin resistant). Following these results, aerothionin was then tested against eight MDR TB clinical isolates with different drug-resistance patterns and nine non-tuberculosis mycobacterial species. All MDR TB isolates were susceptible towards aerothionin with MIC ranging from 6.5 to 25 mg/mL. From the group of non-tuberculosis mycobacteria, three of them were inhibited: *M. avium* (100 mg/mL), *M. scrofulaceum* (100 mg/mL) and *M. kansasii* (50 mg/mL), which indicates a partially selective mode of action against Mtb.[5]

Aerothionin (**1**) turned out to be a very promising Mtb inhibitor, however, calafianin (**28**), despite very similar structure, had no significant activity (**Figure 13**).[5] The only differences between these compounds are 1,2-epoxy- and 3-oxo- group in calafianin instead of 1-hydroxy- and 3-methoxy- group in aerothionin, respectively. For this reason Encarnación et al.[5] suggested that 1-hydroxy-2,4-dibromo-3-methoxy-8-carbamoyl group might be essential for antimycobacterial activity.

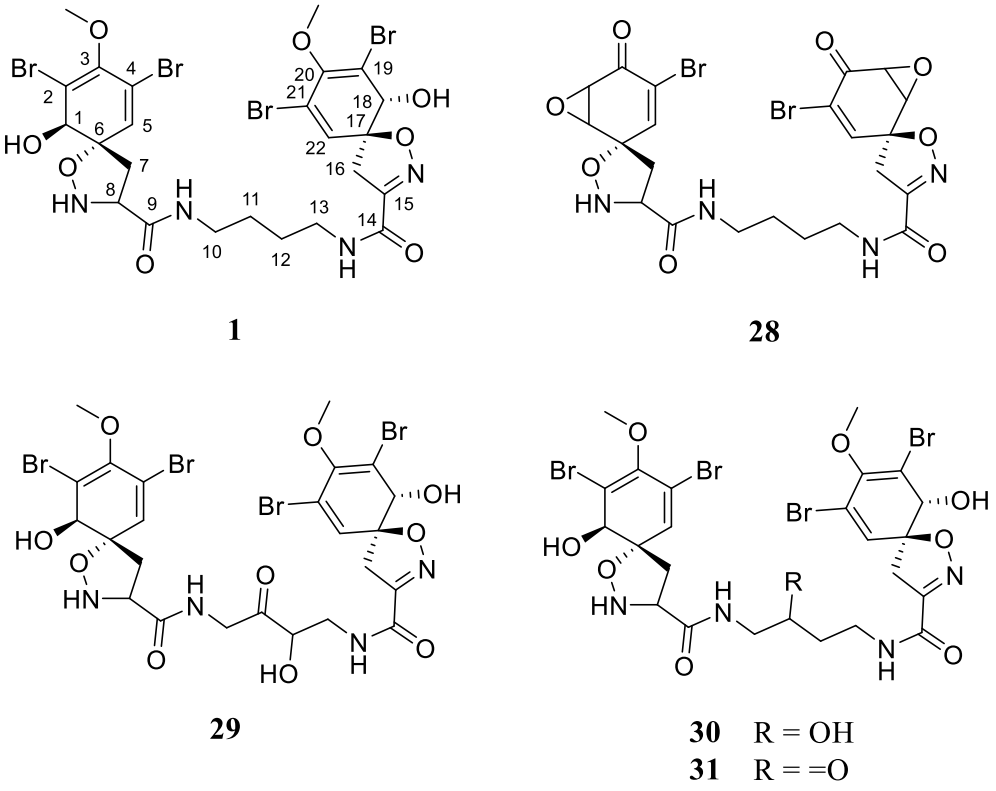

Figure 13: Structures of aerothionin (**1**), calafianin (**28**), 11-oxo-12-epihydroxyaerothionin (**29**), 11-hydroxyaerothionin (**30**) and 11-oxoaerothionin (**31**).

11-oxo-12-epihydroxyaerothionin (**29**) and 11-hydroxyaerothionin (**30**) caused 60 % and 70 % inhibition of Mtb growth, respectively, while 11-oxoaerothionin (**31**) induced

no inhibition at all.[2] El Sayed et al. assumed that hydroxylation at positions 11 or 12 is mutual for the activity of these compounds.[2] This presumption was refuted not only with aerothionin, but also 11-deoxyfistularin-3 (**32, Figure 14**), which are active and both miss the hydroxylation at these positions.[3,5]

Bromotyrosine-derived marine compounds (**33** and **34, Figure 14**) structurally related to aerothionins found in sponge *Oceania sp*. were discovered as the first examples of natural products that inhibit mycobacterial enzyme mycothiol S-conjugate amidase.[4] Compound **33** contains brominated spirocyclohexadienylisoxazoline like aerothionin, but **34** has dibrominated benzene ring and does not contain 1-hydroxy-2,4-dibromo-3-methoxy-8-carbamoyl group, which Encarnación et al.[5] considered mutual for activity against Mtb. This implies that further studies are needed to discover what substitutions in aerothionin are necessary for the mechanism of action.

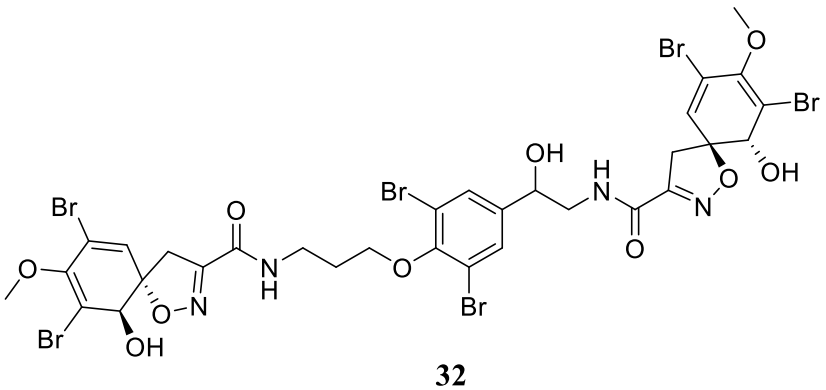

32

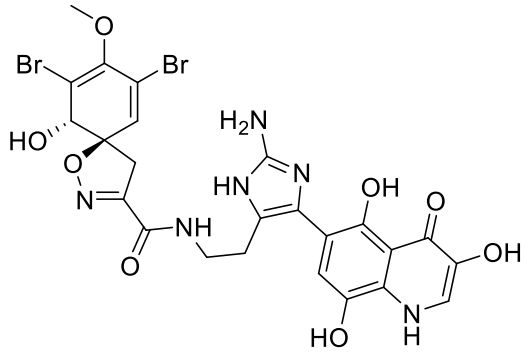

33

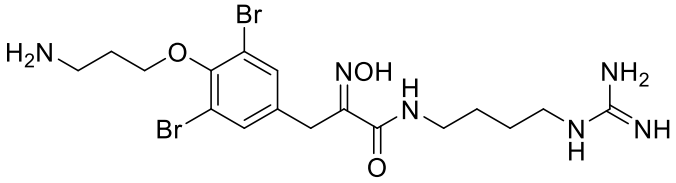

34

Figure 14: Structures of 11-deoxyfistularin-3 (**32**) and compounds **33** and **34**.

5.6 Amide bond formation

Amide bonds play a crucial role in both nature and technology, as they are pervasive not only in peptides, but also in polymers, many natural products (e.g. alkaloids) and pharmaceuticals. Amides are usually synthetised by coupling of carboxylic acids and amines; however, this reaction does not occur spontaneously and typically needs high temperatures (160–180°C), which can be detrimental to other functionalities present in the molecule.[63]

Therefore it is necessary to use a coupling reagent that activates the acid by attaching a leaving group to the acyl carbon of the acid, which allows attack by the amino group[64], or to convert carboxylic acid into a suitable derivative before the reaction.

Because of the huge amount of coupling reagents and synthetic methods, in the following chapters the reaction mechanism of those coupling agents that were used during this research work will be explained; other options will not be discussed.

5.6.1 Carbodiimides

One of the first coupling reagents synthesised.[64] Some of the most frequently used ones are dicyclohexyl carbodiimide (DCC, **35**), diisopropyl carbodiimide (DIC, **36**) and 1-ethyl-3-(3′-dimethylaminopropyl)carbodiimide HCl salt (EDC·HCl, **37**).[63] (**Figure 15**) The efforts have been focused on carbodiimides, which lead to water-soluble ureas, because the ureas formed as a byproduct when using DCC or DIC are sometimes difficult to remove.[64]

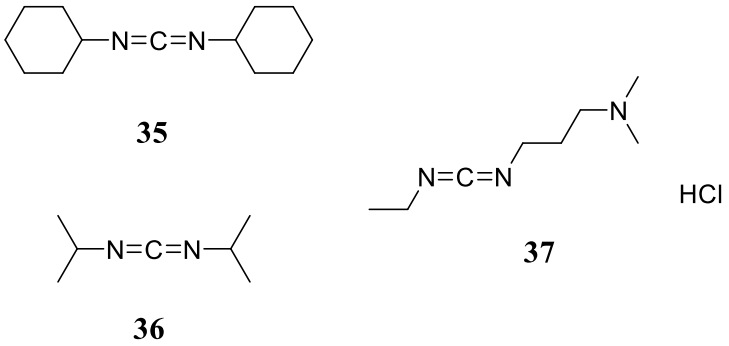

Figure 15: Structures of carbodiimide agents: DCC (**35**), DIC (**36**) and (EDC·HCl, (**37**).

The mechanism for coupling using DCC is shown in **Scheme 1**. The carboxylic acid reacts with DCC to form *O*-acylisourea intermediate, that then reacts with the amine to form the amide: directly, with the byproduct dicyclohexylurea (DCU); or through the

formation of carboxylic acid anhydride. The reaction can also yield *N*-acylurea byproduct; hovewer, this side reaction is significantly reduced when the acid reacts with the coupling reagent at 0°C before the addition of amine.

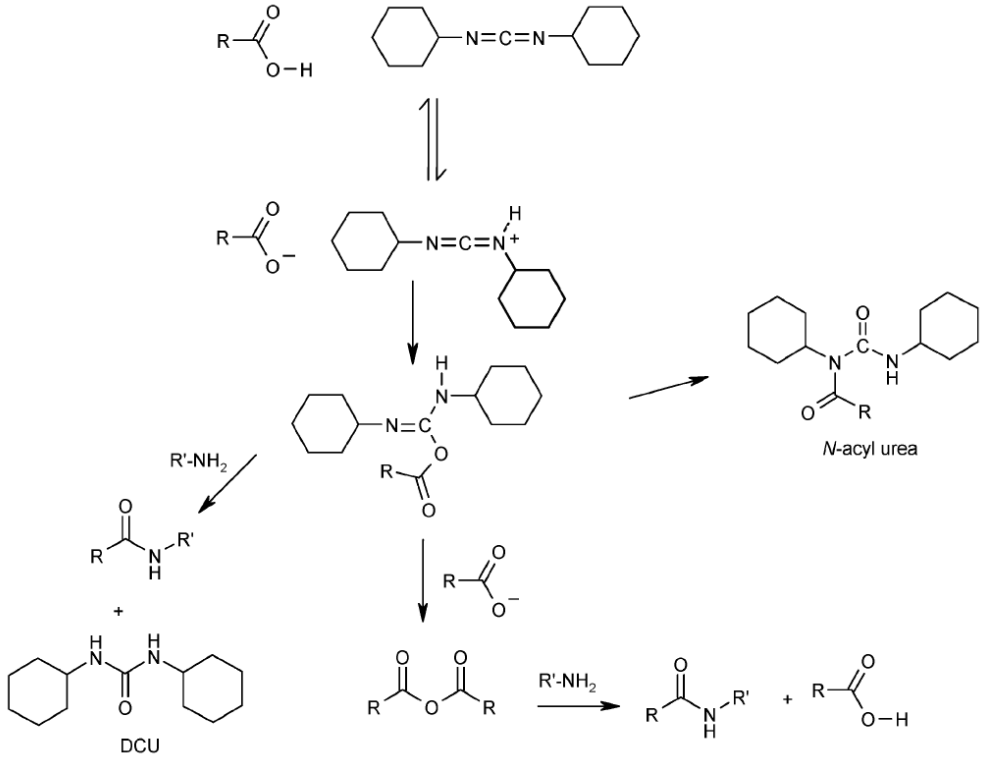

Scheme 1: Coupling using DCC. Taken from Valeur et al.[64]

Another option how to prevent the side reactions and epimerisation is adding a nucleophile that reacts faster than the acyl transfer, while the formed intermediate is still reactive enough to couple with the amine.[63] 4-dimethylaminopyridine (DMAP, **38, Figure 16**) and 1-hydroxy-1*H*-benzotriazole (HOBt, **39**) are examples of such additives. (**Scheme 2 –** the reactive intermediate is OBt (*O*-benzotriazole) active ester.)

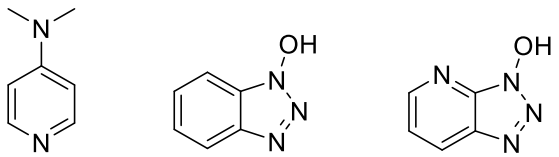

38 **39** **40**

Figure 16: Structures of DMAP (**38**), HOBt, (**39**) and HOAt (**40**).

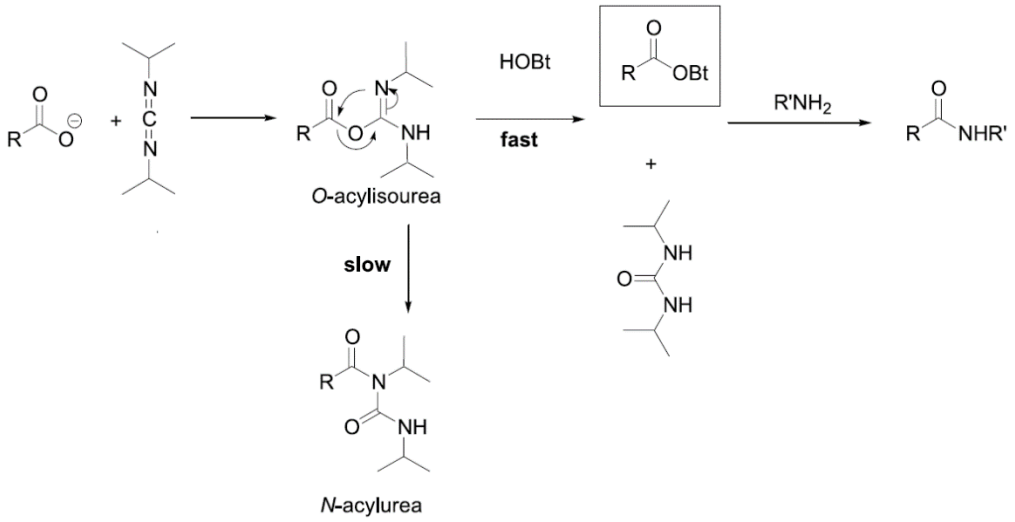

Scheme 2: Use of HOBt to minimise the formation of *N*-acylurea. Taken from Montalbetti et al.[63]

A related additive, 1-hydroxy-7-azabenzotriazole (HOAt, **40**), has been reported by Carpino[65] to be more efficient than HOBt with decreased epimerisation and higher yields. Copper(II) complexes with HOBt or HOAt turned out to be useful additives in lowering the epimerisation as well.[66]

5.6.2 Coupling reagents based on 1H-benzotriazole

These reagents can be divided to uronium/aminium, phosphonium and immonium salts (**Figure 17**).

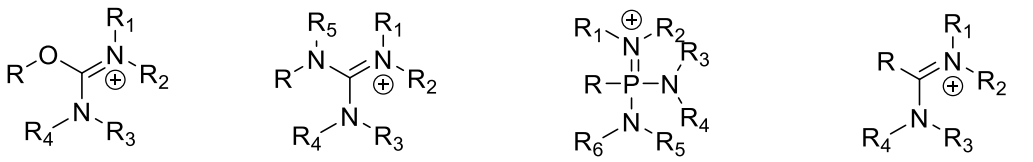

uronium salt | aminium salt | phosphonium salt | immonium salt

Figure 17: Salts associated with reagents based on *1H*-benzotriazole.

5.6.2.1 Uronium/aminium salts

Uronium and aminium salts are in fact isomers and whether these compounds are in *O*-form (uronium) or *N*-form (aminium) depends on the solvent, counter anion and isolation method.[64] (**Figure 18**) They react with the carboxylic acid and form OAt/OBt (At – azabenzotriazole) active esters (**Scheme 3**), that subsequently react with amines.

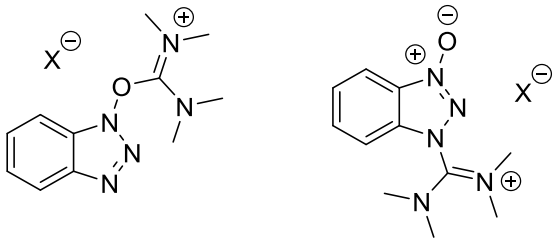

Figure 18: Aminium and uronium isomers.

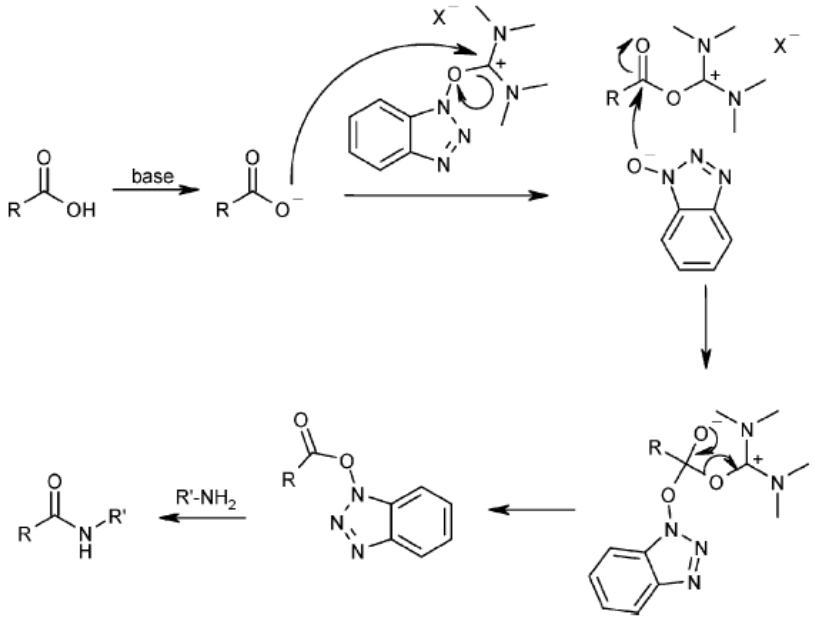

Scheme 3: Coupling using uronium type of reagents. Taken from Valeur et al.[64]

The most common examples are *O*-(1*H*-benzotriazol-1-yl)-*N,N,N′,N′*-tetramethyluronium hexafluorophosphate (HBTU, **41, Figure 19**), it's tetrafluoroborate equivalent TBTU (**42**) and their *N*-forms HATU (1-[bis(dimethylamino)methylene]-1*H*-1,2,3-triazolo[4,5-b]pyridinium 3-oxide hexafluorophosphate, **43**) and TATU (*O*-(7-azabenzotriazol-1-yl)-*N,N,N′,N′*-tetra-methyluronium tetrafluoroborate, **44**).[63] Similarily, Carpino proved that coupling agents based on HOAt are more efficient than those based on HOBt.[67]

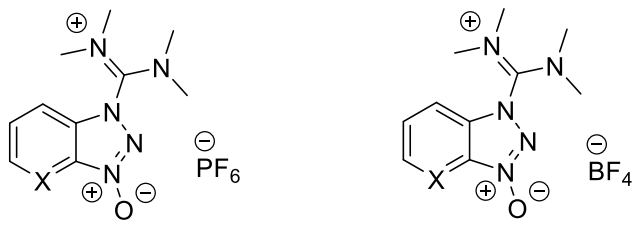

HBTU **41** X = CH
HATU **43** X = N

TBTU **42** X = CH
TATU **44** X = N

Figure 19: Structures of aminium coupling agents.

Disadvantage of uronium/aminium salts is that they also act as guanidylation agents, which leads to guanidinium side products (**Scheme 4**).

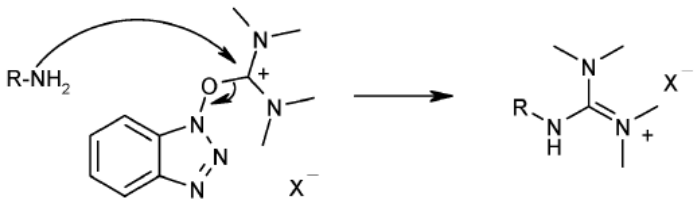

Scheme 4: Guanidinium formation with uronium type of agents. Taken from Valeur et al.[64]

5.6.2.2 Phosphonium salts

The first phosphonium salt introduced was benzotriazol-1-yl-oxy-tris-(dimethylamino)-phosphonium hexafluorophosphate (BOP, **45, Figure 20**), but has been completely replaced by benzotriazol-1-yloxytripyrrolidinophosphonium hexafluorophosphate (PyBOP, **46**) due to the high toxicity associated with the byproduct hexamethylphosphoric triamide (HMPA, **47**) generated during the reaction.[64,68] The acid and amine are mixed in the presence of PyBOP and diisopropylethylamine (DIPEA) or triethylamine Et_3N. PyBOP reacts with the deprotonated acid to form HOBt and activated acyl-phosphonium; HOBt and activated acid then generate a Bt ester, which is subjected to aminolysis (**Scheme 5**).

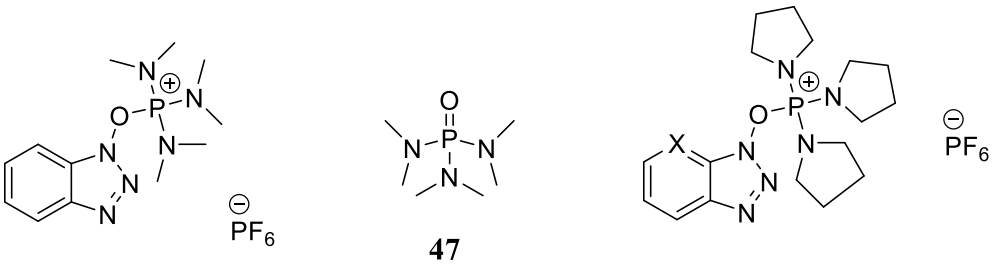

45 **47**

PyBOP **46** X = CH
PyAOP **48** X = N

Figure 20: Structures of phosphonium coupling reagents **45**, **46**, **48** and toxic byproduct HMPA (**47**).

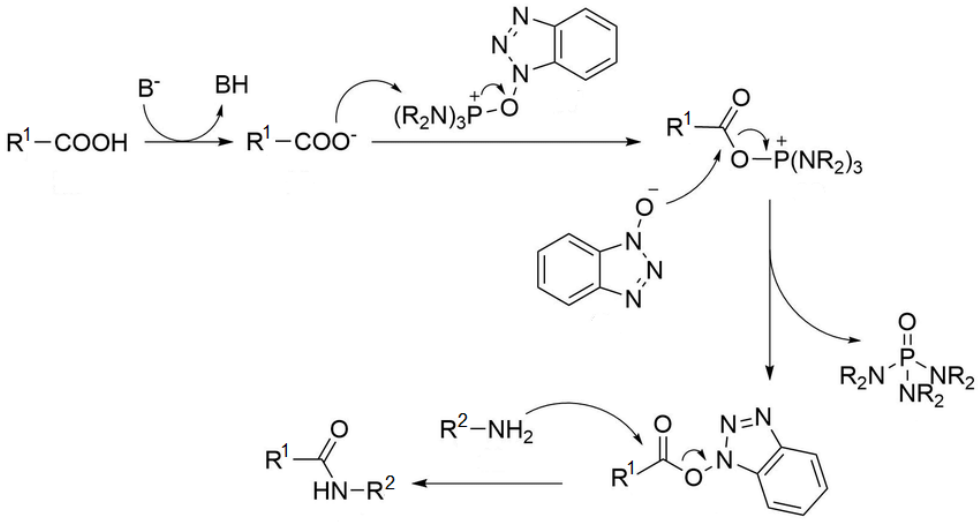

Scheme 5: Coupling mechanism using PyBOP. Taken from Moiola et al.[69]

Again, PyBOP to PyAOP ([7-Azabenzotriazol-1-yloxy]tripyrrolidinophosphonium hexafluorophosphate, **48**) were compared and results showed that aza-derivatives are more active.[70]

5.6.3 Acyl chlorides

This is considered to be one of the easiest methods how to activate the acid and is usually done in two steps. First, carboxylic acid is converted into an acyl halide using oxalyl chloride $(COCl)_2$, thionyl chloride $SOCl_2$, phosphorus trichloride PCl_3, phosphorus pentachloride PCl_5 or phosphorus oxychloride $POCl_3$. The mechanism of reaction using thionyl chloride is shown in **Scheme 6**. These reactions are often catalysed by the addition of a drop of dimethylformamide (DMF) (**Scheme 7**).[63]

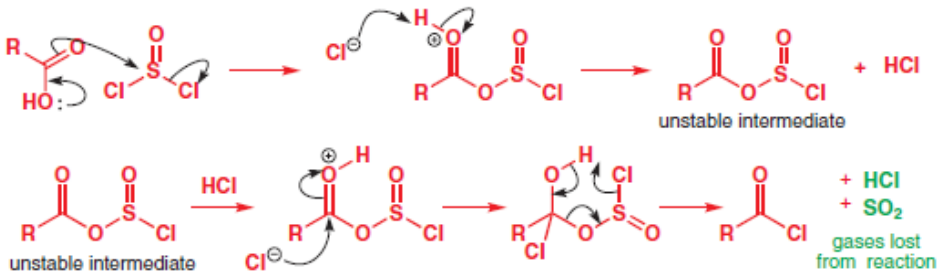

Scheme 6: Mechanism of acyl chloride formation using thionyl chloride. Taken from Clayden et al.[71]

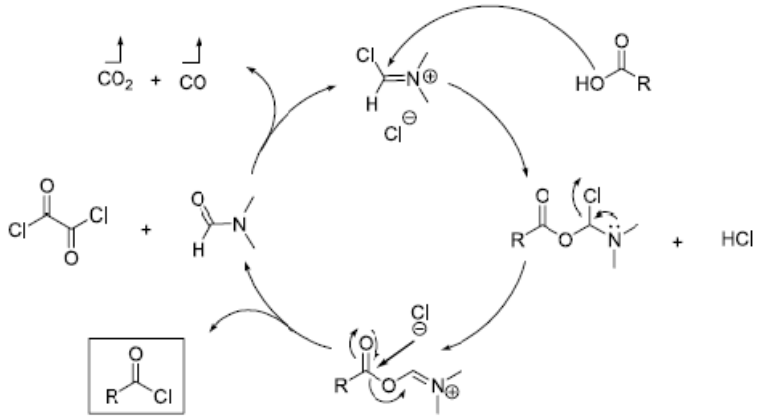

Scheme 7: Activation with DMF – catalytic cycle. Taken from Montalbetti et al.[63]

In the second step, the acyl chloride reacts with the amine to form the amide bond. This reaction can be accelerated by a catalytic amount of DMAP (**Scheme 8**) or pyridine. Pyridine is sometimes used also as a solvent.

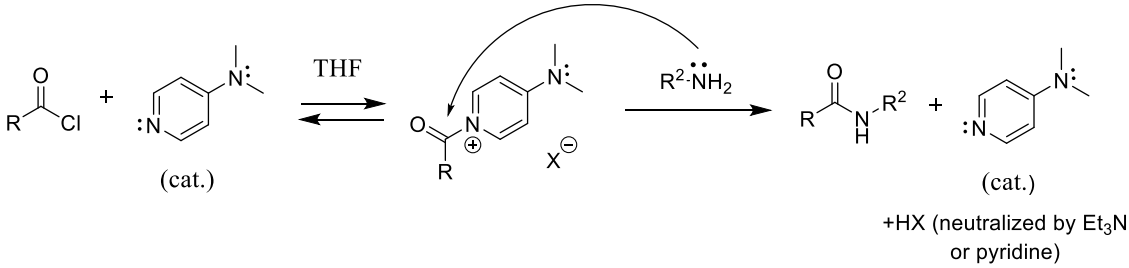

Scheme 8: Mechanism of DMAP catalysis.

One of the disadvantages of the mentioned chlorinating agents is the production of HCl, which can be harmful for some acid sensitive substrates. This can be avoided by carrying out the reaction in the presence of a base – a non-nucleophilic tertiary amine (Et_3N, DIPEA) or *N*-methylmorpholine. The base also prevents the conversion of the amine into its HCl salt.

The main limitations of acyl chlorides include cleavage of protecting groups, racemisation, danger of hydrolysis and other side reactions.[63]

6 EXPERIMENTAL PART

6.1 Laboratory equipment and instruments

All reactions were carried out using commercially available starting materials purchased from Sigma-Aldrich (Schnelldorf, Germany) and Fluorochem (Hadfield, United Kingdom) without further purification, unless otherwise stated. All reactions in anhydrous solvents were performed in oven-dried glassware under an inert atmosphere of dry argon. The progress of chemical reactions was monitored by thin-layer chromatography on Silica Gel 60 F_{254} aluminium sheets acquired from Merck (Darmstadt, Germany), and visualization of the amine compounds was done using ninhydrin (a 0.2 % w/v solution in a 3 % solution of acetic acid in 1-butanol) staining.

The melting points were measured with Stuart SMP40 automated melting point apparatus and are uncorrected.

^{1}H NMR, ^{13}C NMR and ^{15}N NMR spectra in $CDCl_3$, d_6-DMSO, d_6-acetone, CD_3CN or CD_3OD at ambient temperature were recorded on a Bruker Ascend 400 MHz - Avance III HD NMR spectrometer (Bruker Corporation, Billerica, MA, USA). Chemical shifts (δ) are given in parts per million (ppm) relative to the NMR reference solvent signals ($CDCl_3$: 7.26 ppm, 77.16 ppm; CD_3CN: 1.94 ppm, 118.26 ppm; CD_3OD: 3.31 ppm, 49.00 ppm; d_6-DMSO: 2.50 ppm, 39.52 ppm; d_6-acetone: 2.05 ppm, 29.84 ppm). Multiplicities are indicated by s (singlet), br s (broad singlet), d (doublet), dd (doublet of doublets), ddd (doublet of doublet of doublets), t (triplet), dt (doublet of triplets), q (quartet), p (pentet) and m (multiplet). The coupling constants *J* are quoted in hertz (Hz).

LC-MS and HRMS spectra were recorded using Waters Acquity UPLC®-system (with Acquity UPLC® BEH C18 column, 1.7 µm, 50 mm × 2.1 mm, Waters) with Waters Syn-apt G2 HDMS with the ESI (+), high resolution mode. The mobile phase consisted of H_2O (A) and acetonitrile (B) both containing 0.1% formic acid. LRMS were recorded with MS Advion expression® CMS with ASAP and Plate Express TLC reader.

Microwave syntheses were performed in sealed tubes using Biotage Initiator+ SP Wave Microwave Synthesizer instrument equipped with an external IR sensor. The flash chromatography was performed with Biotage Isolera One flash chromatography purification system with 200-800 nm UV-VIS detector using SNAP KP-Sil 5g, 10 g, 25 g or 50 g cartridges.

6.2 Chemistry

In general, synthesis of the compounds consisted of two parts: a synthetic route from L-tyrosine to 7,9-dibromo-8-oxo-1-oxa-2-azaspiro[4.5]deca-2,6,9-triene-3-carboxylic acid **MS-4** (and it's not brominated equivalent **MS-11**) and synthesis of amides.

6.2.1 Synthetic route towards carboxylic acid intermediates

Reactions in **Scheme 1** were performed according to procedure previously developed at the Division of Pharmaceutical Chemistry and Technology[72].

(**Scheme 9**) The first step in preparation of spirocyclic scaffold was esterification of L-tyrosine to L-tyrosine *tert*-butyl ester **MS-1**, which was subsequently oxidized with sodium tungstate to give the oxime **MS-2**. Oxime **2** was subjected to oxidative spirocyclization by treatment with *N*-bromosuccinimide (**MS-3**) or phenyliodine bis(trifluoroacetate) (**MS-9**) to obtain brominated (**MS-3**) or not brominated (**MS-9**) spirocyclic ester, respectively. Finally, hydrolysis of the *tert*-butyl ester by trifluoroacetic acid gave the carboxylic acids **MS-4** and **MS-11**.

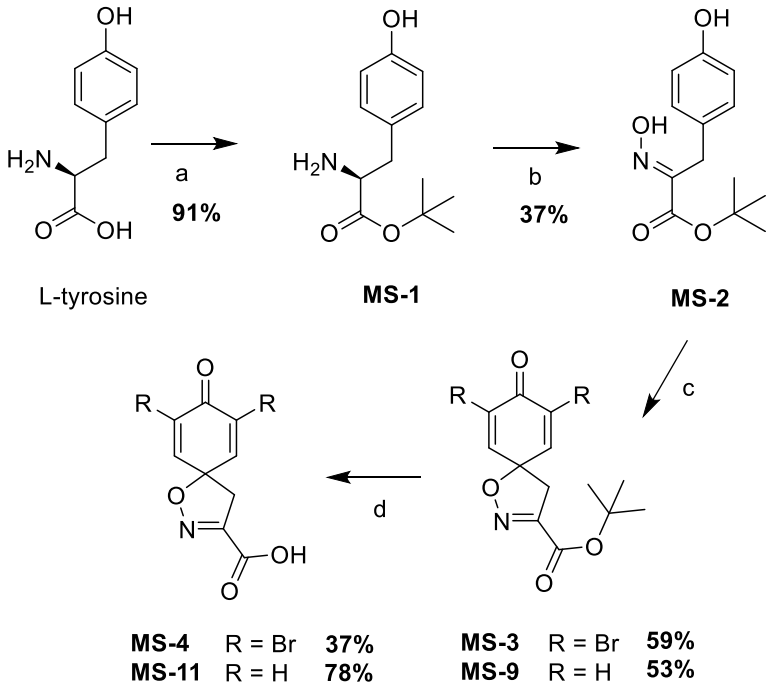

Scheme 9: Synthesis of carboxylic acid intermediates. Reagents and conditions: a) *tert*-butyl acetate, perchloric acid, 0°C, then r.t., 23 h; b) $Na_2WO_4 \cdot 2H_2O$, H_2O_2, ethanol; 24 h, c) PIDA, trifluoroethanol, 0°C, 1 h / NBS; d) TFA, DCM, 20°C, 1.5 h

6.2.2 Amide synthesis

Intermediates **MS-4** and **MS-11** underwent a series of amide couplings with the aim to obtain the final compounds (**Scheme 10**). 7,9-dichloro-8-oxo-1-oxa-2-azaspiro[4.5]deca-2,6,9-triene-3-carboxylic acid (**FV 3**), synthetized by Fiammetta Vitulano at the Division of Pharmaceutical Chemistry and Technology (unpublished data), was used for the synthesis of compound **MS-31**.

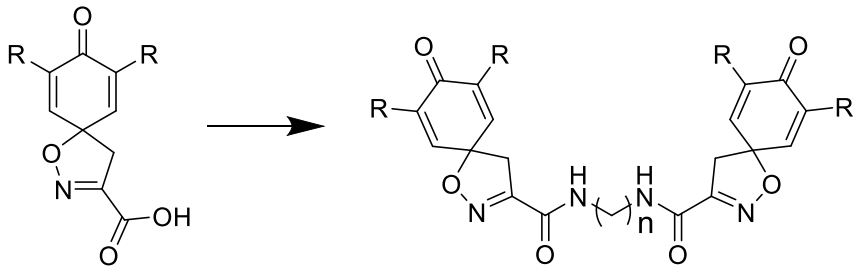

MS-4 R = Br
MS-11 R = H
FV-3 R = Cl

n = 3, 4

Scheme 10: General reaction scheme for the synthesis of final products.

In the beginning, reactions **MS-5**, **MS-8** and **MS-27** were performed according to the procedure previously developed in our laboratory[72]. In case of **MS-5**, 1,4-diaminobutane was added to **MS-4** and then other reagents and solvents. After the addition of the amine whole content of the flask turned black and a gas formation was observed. The mixture was irradiated in the microwave reactor. After the work-up, there was no trace of the desired product. (There is a possibility that an acid-base reaction occurred after the addition of the amine to the acid.)

As a precaution to this occurrence, in reactions **MS-8** and **MS-27** the carboxylic acid was added finally after adding all other reagents (it was impossible to add the amine as the last one, because of its properties – it's slowly melting at room temperature, remaining in semi-solid state). In case of **MS-8**, the mixture was irradiated in the microvawe reactor (60°C, 2 h), while in **MS-27**, the reaction was cooled and only slowly allowed to reach room temperature. The work-up remained the same as in **MS-5**. However, after the purification, the product was not present (according to the NMR).

Therefore, a different protocol, reported by Ogamino and Nishiyama[73], was used. 1,4-Diaminobutane in DMF was treated with **MS-4** in the presence of PyBOP at room

temperature for two days. Unfortunately, when the mixture was checked by NMR, there were no peaks that would imply a presence of the amide bridge in the molecule.

Subsequently, a modified method of Garcia et al.[74] was tried for the synthesis **MS-10**. In this case, active ester of the carboxylic acid forms first and then splits to enable the creation of amide bond. Since the starting material did not completely dissolve (in the mixture of dioxane and methanol) and was still present after leaving the reaction overnight, the temperature was increased to 60°C. After that the compounds dissolved and during the day the solution changed colour to dark brown. The reaction was left until morning. In spite of that, this reaction was also unsuccessful.

In reaction **MS-7** (**Scheme 11**), as an alternative approach (based on aminolysis of ester), a *tert*-butyl ester **MS-3** reacted with amine under conditions reported by Nishiyama and Yamamura[75]. Despite the successful synthesis of aerothionin in the literature, there was no trace of the desired product in the NMR. (Although the cause of the unsuccessful result is not known, one of the reasons could be the steric hindrance of the *tert*-butyl moiety, compared to the methyl group.)

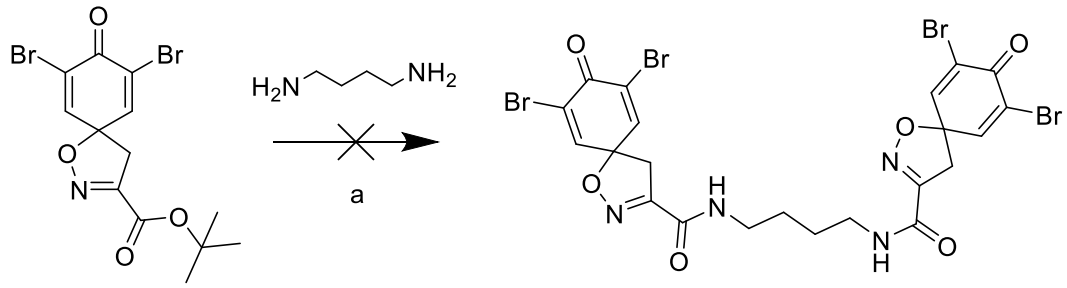

MS-3

Scheme 11: Unsuccessful reaction **MS-7**. Reagents and conditions: a) anh. DCM, anh. DMF, r.t., 40 h

Suspecting that one of the reasons for unsuccessful coupling reactions could be the presence of TFA in the starting material (carboxylic acid), and considering that uronium/aminium salts were reported to give more efficient couplings compared to HOBt[64], one more coupling was executed using HATU in basic conditions (diisopropylethylamine (DIPEA)). This attempt also failed.

For better overview, the reactions are listed in **Table 1**:

Table 1: Unsuccessful coupling reactions.

Reaction code	Amine	Reagents	Temperature	Time	Note
MS-5	1,4-DAB	HOBt, EDC·HCl, anh. DCM	60°C	2 h	microwave; work-up: washed with 1M HCl, saturated solution of NH_4Cl in water, and brine
MS-8	1,4-DAB	HOBt, EDC·HCl, anh. DCM	60°C	2 h	microwave; work-up: washed with 1M HCl, saturated solution of NH_4Cl in water, and brine
MS-27	1,3-DAP	HOBt, EDC·HCl, anh. DCM, Et_3N	0-5°C, then r.t.	24 h	ice, then r.t.; work-up: washed with 1M HCl, saturated solution of NH_4Cl in water, and brine
MS-6	1,4-DAB	PyBOP, DMF	r.t.	48 h	work-up: washed with 1M HCl, saturated solution of NH_4Cl in water, and brine
MS-10	1,3-DAP	*N*-hydroxyphtalimide, DCC, Et_3N, dioxane/ methanol (10:1)	r.t., then 60°C	48 h	no work-up, purified with flash chromatography
MS-7	1,4-DAB	anh. DCM, anh. DMF	r.t.	40 h	work-up: washed with H_2O and brine, then purified with flash chromatography
MS-18	1,3-DAP	HATU, DIPEA, anh. DMF	0–5°C, then r.t.	24 h	no work-up

At this point, facing the difficulty of coupling both amino groups at the same time, we turned to longer, stepwise strategy using commercially available Boc-protected diamine derivatives.

Firstly, a coupling protocol previously used in the synthesis **MS-10**[72] was performed with *N*-Boc-1,3-diaminopropane (reaction **MS-14**, **Scheme 12**). The only differences

were using EDC·HCl instead of dicyclohexylcarbodiimide (DCC), seeing the possible problem of contaminating the product with a by-product *N,N'*-dicyclohexylurea (DCU), which can be difficult to remove[76], and a bigger amount of triethylamine, as a precaution of rest of TFA present in **MS-4** that could interfere with the reaction. Because of the insolubility of *N*-hydroxyphtalimide and EDC·HCl in dioxane/methanol solution, the temperature was increased to 55°C. After 24 hours the solvent was evaporated and the mixture purified with automated flash chromatography (twice, as long as after the first purification there were so many peaks in NMR that it was impossible to distinguish them). Unfortunately, this reaction didn't lead to the product either.

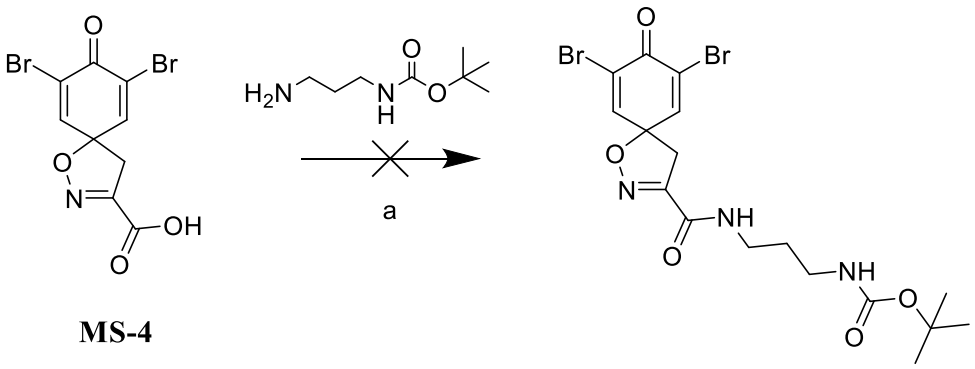

Scheme 12: Unsuccessful reaction **MS-14**. Reagents and conditions: a) N-hydroxyphtalimide, EDC·HCl, Et_3N, anh. dioxane, anh. methanol (dioxane:methanol 11:1); 55°C, 24 h

Then, procedure using HOBt and EDC·HCl was used[72] (**Scheme 13**), affording an intermediate product (**MS-15**), however, in poor yield (26 %). Deprotection was carried out by TFA in DCM, without further purification (just evaporating the solvent) assuming that free NH_2 group could cause the product to stay attached to the silica. Subsequently, the deprotected intermediate reacted with **MS-4** in the second coupling, which, unexpectedly, turned out to be unsuccessful.

MS-11 was analogically subjected to HOBt and EDC mediated coupling (**Scheme 14**) (also in poor yield: 17 %), followed by deprotection with TFA and another coupling, finally allowing to obtain a desired product (50 %).

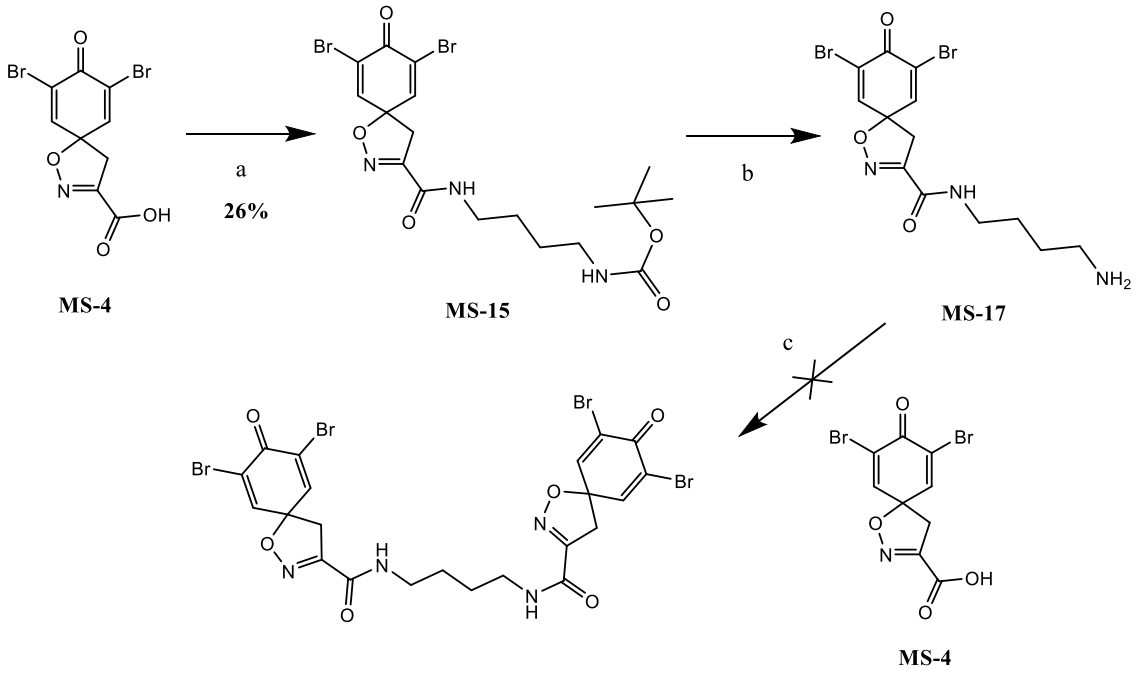

Scheme 13: Unsuccessful synthesis with HOBt and EDC·HCl. Reagents and conditions: a) *N*-Boc-1,4-diaminobutane, HOBt, EDC·HCl, Et_3N, anh. DCM, 0–5°C, then r.t., 24 h; b) TFA, anh. DCM, 18 hours, r.t.; c) HOBt, EDC·HCl, Et_3N, anh. DCM, anh. THF, anh. DMF, 0–5°C, then r.t., 27 h

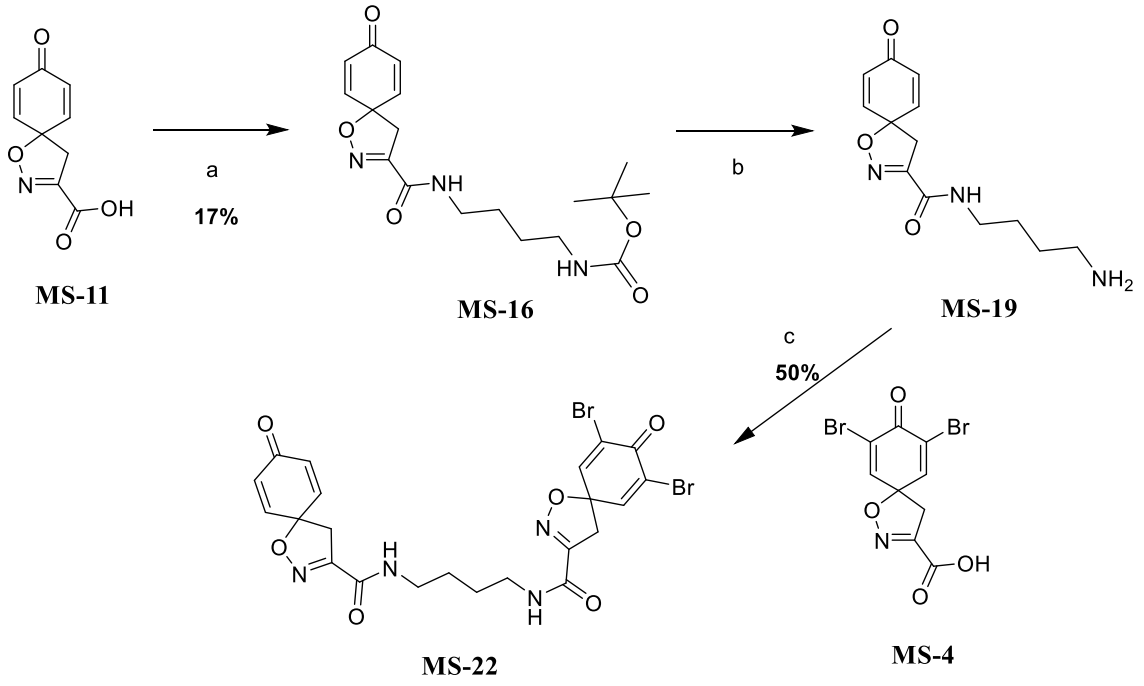

Scheme 14: Successful synthesis with HOBt and EDC·HCl. Reagents and conditions: a) *N*-Boc-1,4-diaminobutane, HOBt, EDC·HCl, Et_3N, anh. DCM, 0–5°C, then r.t., 24 h; b) TFA, anh. DCM, 18 h, r.t.; c) HOBt, EDC·HCl, Et_3N, anh. DCM, anh. THF, anh. DMF, 0–5°C, then r.t., 48 h.

After this, seeing the poor yields in HOBt/EDC couplings and many fails, we opted for a different approach[77]. The carboxylic acid was converted into acyl chloride (**MS-4a**, **MS-11a**), the solvent was evaporated and the corresponding acyl chloride was used directly in the next step to achieve mono-substituted intermediates (**MS-15**, **MS-20**, **MS-24**) (**Scheme 15**). However, during the purifications, some impurity co-eluted with the products and therefore it was impossible to obtain them in completely pure form. Nevertheless, the impure intermediates **MS-15**, **MS-20** and **MS-24** reacted with TFA resulting in compounds **MS-17, MS-23** and **MS-26** with free NH_2-group. Despite the fact that **MS-15**, **MS-20** and **MS-24** were not 100 % pure it was clear that this method leads to higher yields compared to HOBt/EDC mediated coupling (e.g. compound **MS-15**: 60 % yield using acyl chlorides and 26 % yield with HOBt/EDC).

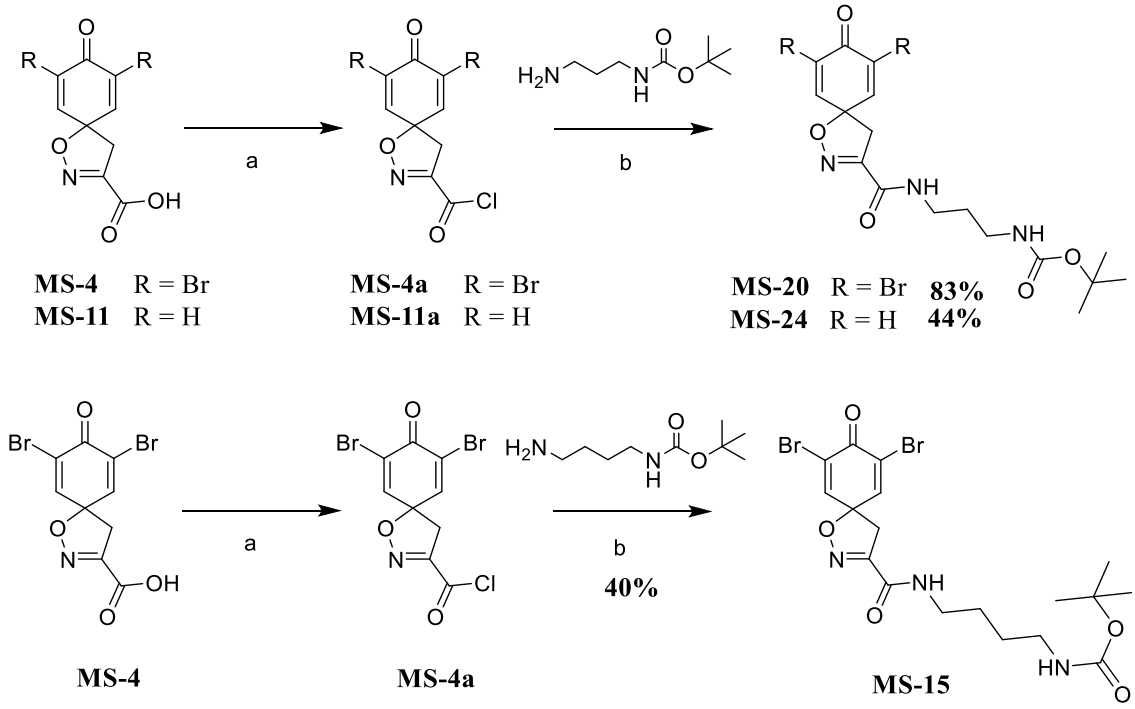

Scheme 15: Synthesis of monosubstituted amides using $(COCl)_2$. Reagents and conditions: a) $(COCl)_2$, anh. DMF (cat.), anh. DCM, anh. THF (DCM : THF 1:1), r.t., 1 h; b) Et_3N, anhydrous DCM, anhydrous THF, r.t., 21 h.

Generally, the mono-substituted intermediates were not purified after the Boc-deprotection, because of the high risk that the compound would stay attached to the silica during chromatography column. However, we tried to purify one third of compound **MS-23** using a SCX-2 ion exchange column. Crude product was dissolved in methanol and put on the column that was previously wetted with MeOH. The column was flushed with 3 column volumes of MeOH, after that with 2M solution of NH_3 in

MeOH, until no more compounds were seen in the fractions on the TLC. Nonetheless, NMR did not confirm the desired product, which implies that the product either stayed stuck in the column or reacted with the NH_3.

Remaining two thirds of **MS-23** were subjected to second coupling.

Then, a series of experiments followed (**Schemes 16, 17, 18, 19**), where the mono-substituted derivatives reacted with carboxylic acid[78] **MS-4** or acyl-chlorides[77] (**MS-4a**, **MS-11a**, **FV-3a**) in order to find the best method how to obtain the final products. However, for an unknown reason, reactions with brominated acid/acyl chloride failed at the final step, whereas reactions with chlorinated and not-substituted acyl chlorides were successful.

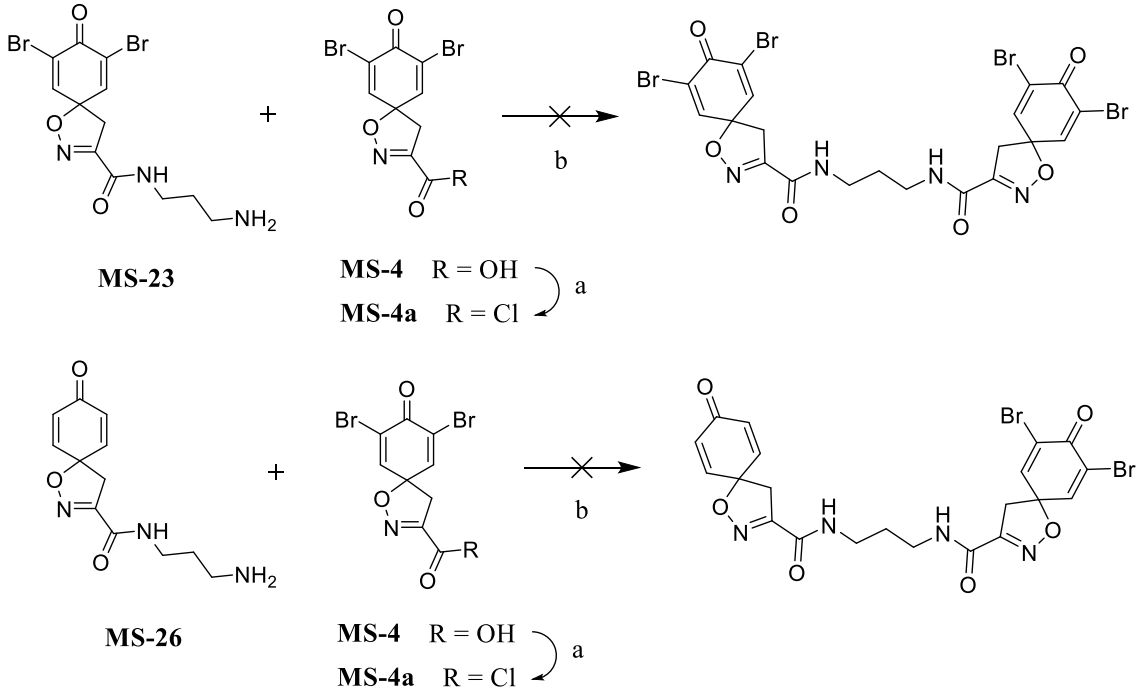

Scheme 16: Unsuccessful syntheses 1. Reagents and conditions: a) $(COCl)_2$, anh. DMF (cat.), anh. THF, r.t., 1 h; b) Et_3N, anh. THF, anh. DMF, r.t., 24 h.

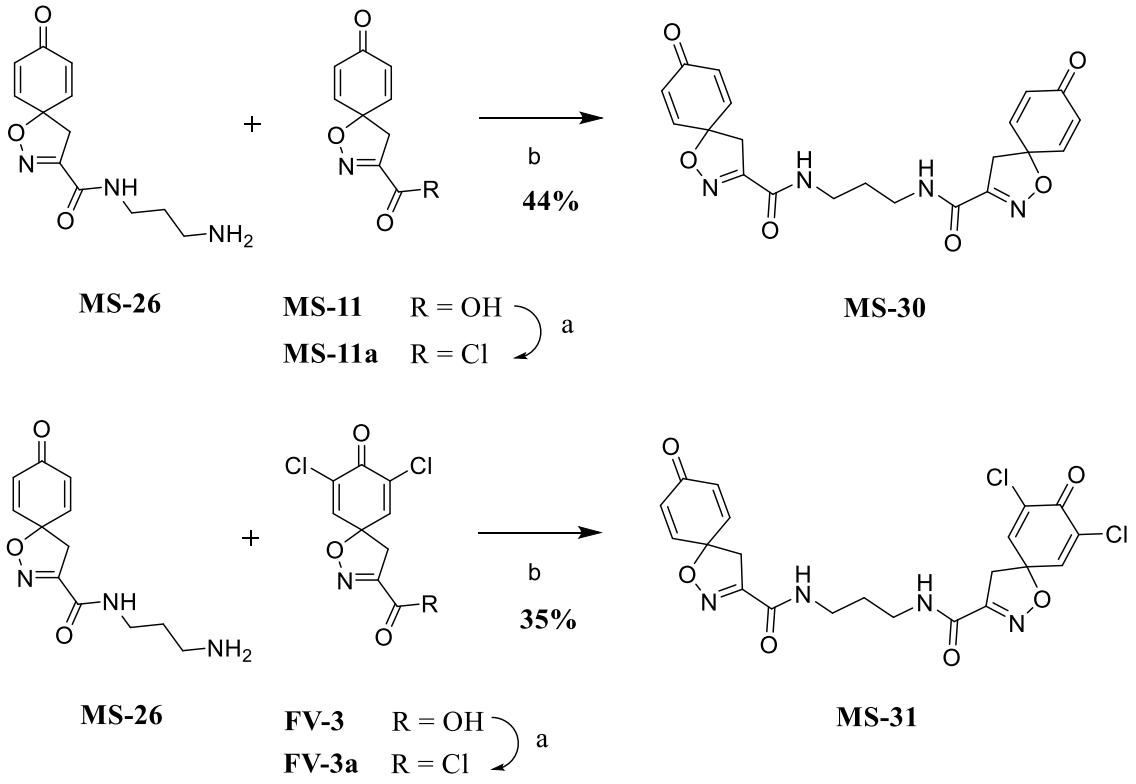

Scheme 17: Synthesis of compounds **MS-30** and **MS-31**. Reagents and conditions: a) $(COCl)_2$, anh. DMF (cat.), anh. THF, r.t., 1 h; b) Et_3N, anh. THF, anh. DMF, r.t., 24 h.

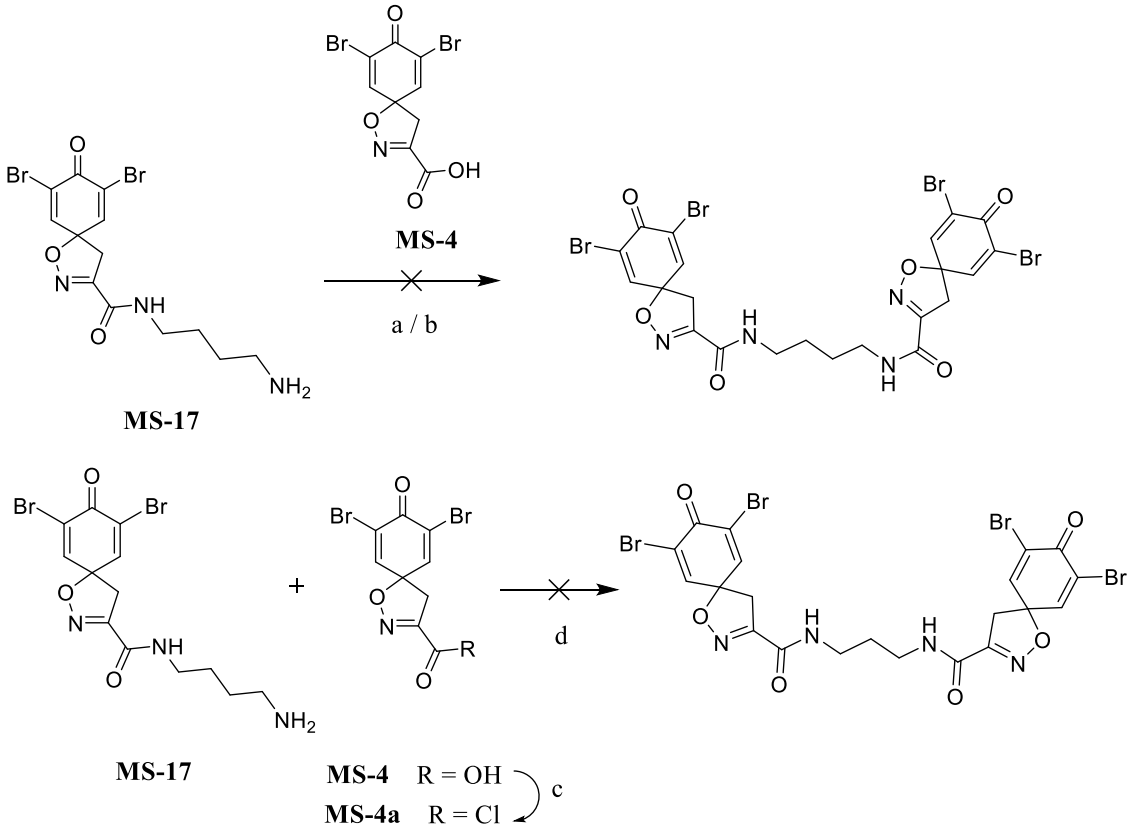

Scheme 18: Unsuccessful syntheses 2. Reagents and conditions: a) DMAP, EDC·HCl, Et_3N, anh. DCM, anh. DMF, 0–5°C, then r.t., 39 h; b) HOBt, EDC·HCl, Et_3N, anh. DCM, anh. DMF, 0–5°C, then r.t., 39 h; c) $(COCl)_2$, anh. DMF (cat.), anh. THF, r.t., 1 h; b) Et_3N, anh. THF, anh. DMF, r.t., 39 h.

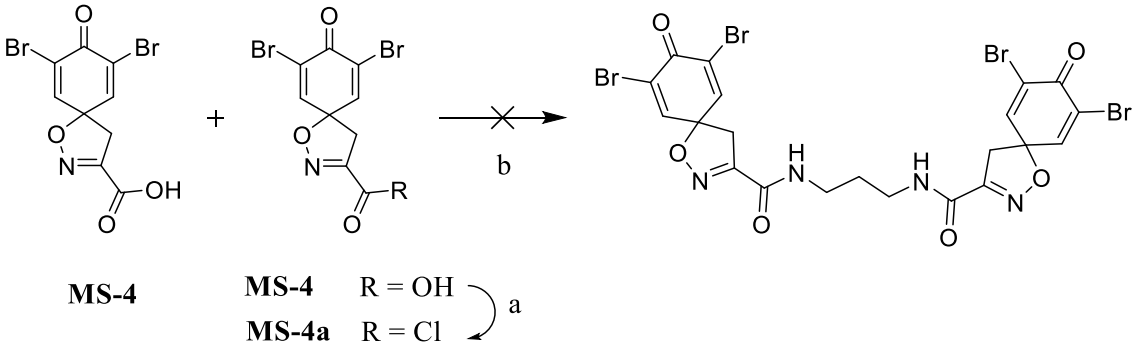

Scheme 19: Unsuccessful synthesis 3. Reagents and conditions: a) $(COCl)_2$, anh. DMF (cat.), anh. THF, r.t., 1 h; b) 1,3-DAP, DMAP, EDC·HCl, Et_3N, anh. DCM, 0–5°C, then r.t., 24 h, after adding **MS-4a** another 24 h.

6.3 Synthetic procedures and analytical data of the prepared compounds

6.3.1 tert-butyl L-tyrosinate (MS-1)

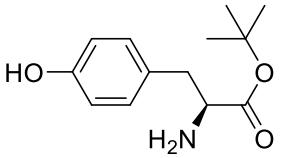

Chemical Abstracts Service (CAS) number: 16874-12-7. L-tyrosine (5.00 g, 27.6 mmol) was suspended in *tert*-butyl acetate (50 mL) in a 250 -mL round-bottomed flask in an ice bath (0°C), then perchloric acid was added dropwise (2.5 ml, 41.4 mmol, 1.5 eq.). The reaction mixture was stirred at room temperature for 23 hours. The mixture was washed with H_2O (40 mL) and a 1M solution of HCl in H_2O (40 mL). The aquous phase was diluted with H_2O (100 mL) followed by an addition of solid K_2CO_3 until the ph was 9. The solution was extracted with EtOAc (3 x 50 mL), the combined organic phases were washed with brine (50 mL), dried over Na_2SO_4, filtered and concentrated *in vacuo*. The brine phase was filtered and washed with water, then dried under reduced pressure. Both portions were combined to give the product. White solid, 5.99 g (91 %). APCI-MS: $[M-H]^-$ m/z 236. ^{1}H NMR (400 MHz, $CDCl_3$) δ 7.03 (d, J = 8.4 Hz, 2H), 6.67 (d, J = 8.5 Hz, 2H), 3.59 (dd, J = 7.7, 5.4 Hz, 1H), 3.13 (s, 2H), 3.00 (dd, J = 13.8, 5.3 Hz, 1H), 2.77 (dd, J = 13.8, 7.8 Hz, 1H), 1.45 (s, 9H). ^{13}C NMR (101 MHz, $CDCl_3$) δ 174.3, 155.2, 130.6, 128.7, 115.7, 81.7, 56.3, 40.1, 28.2. The spectra corresponds to the earlier published spectra[72].

6.3.2 tert-butyl (E)-2-(hydroxyimino)-3-(4-hydroxyphenyl)propanoate (MS-2)

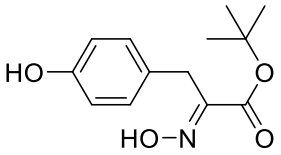

CAS: 2031238-44-3. *Tert*-butyl L-tyrosinate (**MS-1**) (5.99 g, 25.3 mmol) was dissolved in EtOH (100 mL) in a 250 -mL round-bottomed flask and put in an ice bath (0°C). $Na_2WO_4 \cdot 2H_2O$ (9.18g, 27.8 mmol, 1.1 eq.), H_2O_2 (30 %, 45 mL) and H_2O (70 mL) were added to the solution. The mixture was stirred for 24 hours and slowly allowed to reach room temperature. The mixture was diluted with EtOAc (125 mL) and washed

with Na_2SO_3 (10%, 2 x 75 mL), H_2O (2 x 75 mL) and brine (75 mL). Water phase was extracted with EtOAc (3 x 100 mL) and combined organic phase was washed with brine (50 mL), dried over Na_2SO_4, filtered and concentrated *in vacuo*. Yellow solid, crude yield 3.83 g (60 %). The product was purified with automated flash chromatography (heptane/EtOAc 0→100 %). Yellow solid, 2.37 g (37 %). APCI-MS: $[M+H]^+$ m/z 252. ^{1}H NMR (400 MHz, CD_3OD) δ 7.11 – 7.05 (m, 1H), 6.70 (d, J = 8.5 Hz, 1H), 3.79 (s, 1H), 1.43 (s, 6H). ^{13}C NMR (101 MHz, CD_3OH) δ 164.7, 157.0, 153.6, 131.0, 128.7, 116.1, 83.3, 30.3, 28.2. The spectra corresponds to the earlier published spectra[72].

6.3.3 tert-butyl 7,9-dibromo-8-oxo-1-oxa-2-azaspiro[4.5]deca-2,6,9-triene-3-carboxylate (MS-3)

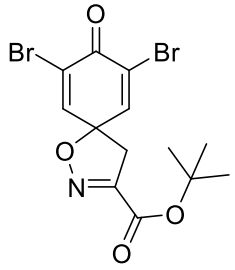

CAS: 2031238-45-4. *Tert*-butyl (*E*)-2-(hydroxyimino)-3-(4-hydroxyphenyl)propanoate (**MS-2**) (1.00 g, 3.98 mmol) was dissolved in anhydrous DMF (10 mL) in a two-necked round-bottomed flask and put in an ice bath (0°C). *N*-bromosuccinimide (2.3 g, 12.9 mmol, 3.25 eq.) in anhydrous DMF (8.5 mL) was added dropwise (15 min.) to this solution. After 40 minutes the mixture was diluted with Et_2O (40 mL), washed with H_2O (2 x 25 mL) and $Na_2S_2O_3$ (10%, 2 x 25 mL). The water phase was back-extracted with Et_2O (2 x 50 mL). Combined organic phases were washed with brine (2 x 35 mL), dried over Na_2SO_4, filtered and concentrated *in vacuo*. Orange solid, crude yield 1.38 g (85 %). The crude was purified with automated flash chromatography (isocratic DCM). White solid, yield 0.96 g (59 %). APCI-MS: $[M+H]^+$ m/z 408, 410. ^{1}H NMR (400 MHz, $CDCl_3$) δ 7.32 (s, 2H), 3.42 (s, 2H), 1.59 (s, 9H). ^{13}C NMR (101 MHz, $CDCl_3$) δ 171.5, 158.3, 152.6, 144.5, 123.9, 86.1, 85.0, 43.5, 28.1. The spectra corresponds to the earlier published spectra[72].

6.3.4 7,9-dibromo-8-oxo-1-oxa-2-azaspiro[4.5]deca-2,6,9-triene-3-carboxylic acid (MS-4)

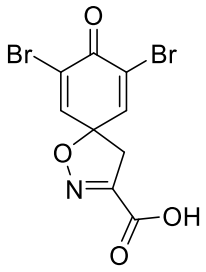

CAS: 90278-50-5. Trifluoroacetic acid (8.4 mL) was added dropwise to a solution of *tert*-butyl 7,9-dibromo-8-oxo-1-oxa-2-azaspiro[4.5]deca-2,6,9-triene-3-carboxylate (**MS-3**) (0.76 g, 1.9 mmol) in anhydrous DCM (10 mL) in a two-neck round-bottomed flask. The mixture was stirred at room temperature for 1.5 h. The solvent was removed *in vacuo*. Light orange solid, yield 0.59 g (90 %). 75 mg were used for reaction MS-5. The rest was purified with automated flash chromatography (DCM/MeOH 0→50 %). Off-white solid, yield 0.24 g (37 %). APCI-MS: $[M+H]^+$ m/z 351. ^{1}H NMR (400 MHz, d_6-Acetone) δ 7.74 (s, 2H), 3.70 (s, 2H). ^{13}C NMR (101 MHz, d_6-Acetone) δ 172.3, 160.7, 153.6, 146.9, 123.2, 87.3, 43.7. The spectra corresponds to the earlier published spectra[72].

6.3.5 tert-butyl 8-oxo-1-oxa-2-azaspiro[4.5]deca-2,6,9-triene-3-carboxylate (MS-9)

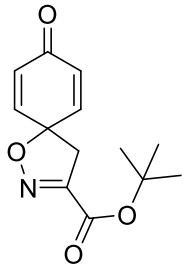

CAS: 294207-83-3. *Tert*-butyl (*E*)-2-(hydroxyimino)-3-(4-hydroxyphenyl)propanoate (**MS-2**) (1.37 g, 5.5 mmol) was dissolved in trifluoroethanol (30 mL) in a two-necked round-bottomed flask (did not dissolve completely), followed by addition of anhydrous pyridine (880 µL, 10.9 mmol, 2 eq.). The flask was put in ice bath (0°C) for 5 min. Phenyliodine bis(trifluoroacetate) (2.58 g, 6.0 mmol, 1.1 eq.) was added to the flask and mixture was stirred for 1.5 h. Reaction was quenched with aqueous $Na_2S_2O_3$ (10 %, 40 mL) and extracted with EtOAc (3 × 45 mL). Combined organic phases were washed

with brine, dried over Na_2SO_4, filtered and concentrated *in vacuo*. Brown oil, crude yield 2.02 g (149 %). The product was purified with automated flash chromatography (heptane/EtOAC 0→100 %). Yellow oil, 0.72 g (53 %). APCI-MS: $[M+H]^+$ m/z 250. ^{1}H NMR (400 MHz, d_6-Acetone) δ 7.20 (d, J = 10.1 Hz, 2H), 6.31 (d, J = 10.1 Hz, 2H), 3.60 (s, 2H), 1.61 (s, 9H). The spectra corresponds to the earlier published spectra[72].

6.3.6 8-oxo-1-oxa-2-azaspiro[4.5]deca-2,6,9-triene-3-carboxylic acid (MS-11)

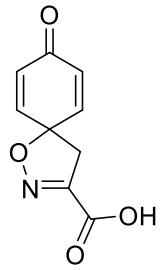

CAS: 88598-41-8. Trifluoroacetic acid (11 mL) was added dropwise to a solution of *tert*-butyl 8-oxo-1-oxa-2-azaspiro[4.5]deca-2,6,9-triene-3-carboxylate (**MS-9**) (0.72 g, 2.9 mmol) in anhydrous DCM (10.5 mL) in a two-neck round-bottomed flask. The mixture was stirred at room temperature for 4.5 h. The solvent was removed *in vacuo*. Brown solid, 0.55 g (99 %). The crude product was purified with automated flash chromatography (DCM/MeOH 0→60 %). Brown solid, 0.43 g (78 %). APCI-MS: $[M+H]^+$ m/z 194. ^{1}H NMR (400 MHz, d_6-Acetone) δ 7.16 – 7.09 (m, 2H), 6.27 – 6.20 (m, 2H), 3.52 (s, 2H). ^{13}C NMR (101 MHz, d_6-Acetone) δ 185.32, 161.47, 153.41, 146.09, 129.70, 84.25, 44.53. The spectra corresponds to the earlier published spectra[72].

6.3.7 tert-butyl (3-(7,9-dibromo-8-oxo-1-oxa-2-azaspiro[4.5]deca-2,6,9-triene-3-carboxamido)propyl)carbamate (MS-15)

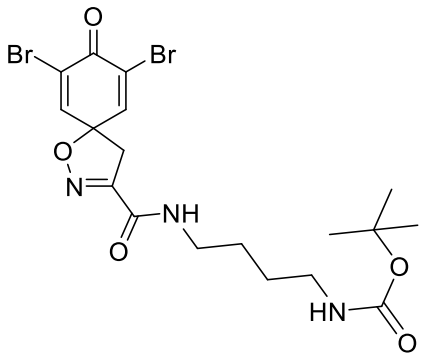

Method A: HOBt (3 mg, 0.02 mmol, 0.1 eq) and EDC·HCl (40 mg, 0.2 mmol, 1.1 eq) were added to a stirred solution of 7,9-dibromo-8-oxo-1-oxa-2-azaspiro[4.5]deca-2,6,9-triene-3-carboxylic acid (**MS-4**) (70 mg, 0.2 mmol) in anhydrous DCM (4 mL) in a two-neck round-bottomed flask at 0–5°C and stirred for 15 min. After this, *N*-Boc-1,4-diaminobutane (40 mg, 0.2 mmol, 1 eq) was added. The reaction mixture was allowed to reach room temperature and stirred for 24 h. The mixture was diluted with DCM (10 mL) and washed with 1M HCl (5 mL), a saturated solution of $NaHCO_3$ in H_2O (5 mL) and brine (5 mL). The organic layer was dried over Na_2SO_4, filtered and concentrated *in vacuo*. Brown solid, raw yield: 80 mg (79 %). The crude product was purified by automated flash chromatography (DCM/MeOH 0→10 %). White solid, 28 mg (26 %).

Method B: Et_3N (596 µL, 4.3 mmol, 3 eq.) was added to a solution of *N*-Boc-1,4-diaminobutane (349 mg, 1.9 mmol, 1.3 eq) in anhydrous THF (10 mL) in a two-neck round-bottomed flask (amine dissolved completely after Et_3N was added). Then acyl chloride **MS-4a** (1 eq) was added dropwise in a mixture of DCM and THF (1:1, 8 mL). The mixture was stirred for 21 hours at room temperature, after that the solvent was removed in *vacuo*. The crude product (brown solid, 340 mg, quant.) was purified with automated flash chromatography (heptane/EtOAc 30→100 %). Yellow solid, 447 mg (60 %). APCI-MS: $[M-H]^-$ m/z 520. ^1H NMR (400 MHz, d_6-Acetone) δ 7.72 (s, 2H), 3.65 (s, 2H), 3.37 – 3.30 (m, 2H), 3.11 – 3.03 (m, 2H), 1.65 – 1.50 (m, 4H).

6.3.8 tert-butyl (3-(8-oxo-1-oxa-2-azaspiro[4.5]deca-2,6,9-triene-3-carboxamido)propyl)carbamate (MS-16)

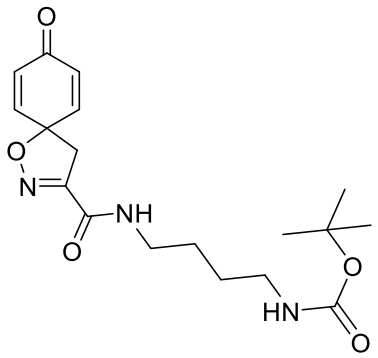

HOBt (5 mg, 0.04 mmol, 0.1 eq) and EDC·HCl (90 mg, 0.5 mmol, 1.1 eq) were added to a stirred solution of 8-oxo-1-oxa-2-azaspiro[4.5]deca-2,6,9-triene-3-carboxylic acid (**MS-11**) (80 mg, 0.4 mmol) in anhydrous DCM (6 mL) in a two-neck round-bottomed flask at 0–5°C and stirred for 15 min. After this, *N*-Boc-1,4-diaminobutane (80 mg, 0.4

mmol, 1 eq) was added. The reaction mixture was allowed to reach room temperature and stirred for 24 h. The mixture was diluted with DCM (10 mL) and washed with 1M HCl (5 mL), a saturated solution of $NaHCO_3$ in H_2O (5 mL) and brine (5 mL). The organic layer was dried over Na_2SO_4, filtered and concentrated *in vacuo*. Brown solid, raw yield: 90 mg (57 %). The crude product was purified by automated flash chromatography (heptane/EtOAc 30→100 %). White solid, 26 mg (17 %). APCI-MS: $[M+H]^-$ m/z 364. 1H NMR (400 MHz, d_6-Acetone) δ 7.71 (s, 1H), 7.12 (d, J = 10.1 Hz, 2H), 6.21 (d, J = 10.03 Hz, 2H), 6.01 (s, 1H), 3.52 (s, 2H), 3.29 (q, J = 6.6 Hz, 2H), 3.11 (q, J = 6.5 Hz, 2H), 1.71 – 1.52 (m, 4H), 1.40 (s, 9H). 13C NMR (101 MHz, d_6-Acetone) δ 185.0, 159.6, 156.7, 155.3, 146.0, 129.1, 82.9, 78.4, 44.4, 40.7, 39.7, 28.7, 28.2, 27.5.

6.3.9 General procedure for Boc-deprotection with TFA (MS-17, MS-19, MS-23, MS-26):

Trifluoroacetic acid was added dropwise to a stirred solution of Boc-protected compound in anhydrous DCM in a two-neck round-bottomed flask (DCM: TFA 2:1, excess). The mixture was stirred at room temperature for 5 h, after that the solvent was removed *in vacuo*.

6.3.10 7,9-dibromo-8-oxo-N-(4-(8-oxo-1-oxa-2-azaspiro[4.5]deca-2,6,9-triene-3-carboxamido)butyl)-1-oxa-2-azaspiro[4.5]deca-2,6,9-triene-3-carboxamide (MS-22)

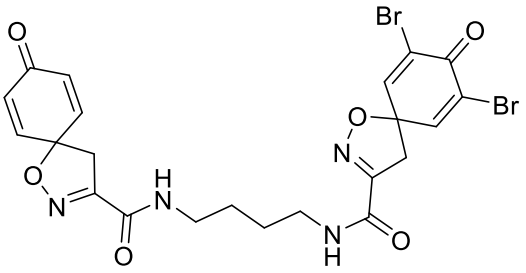

HOBt (1 mg , 0.07 mmol, 0.1 eq) and EDC·HCl (15 mg, 0.08 mmol, 1.1 eq) were added to a stirred solution of 7,9-dibromo-8-oxo-1-oxa-2-azaspiro[4.5]deca-2,6,9-triene-3-carboxylic acid (**MS-4**) (30 mg, 0.8 mmol, 1.1 eq) in anhydrous DCM (5 mL) in a two-neck round-bottomed flask at 0–5°C and stirred for 15 min. After this, *N*-(4-aminobutyl)-8-oxo-1-oxa-2-azaspiro[4.5]deca-2,6,9-triene-3-carboxamide (**MS-19)** (18 mg, 0.07 mmol, 1 eq) in a mixture of DMF and THF (2:1, 1.5 mL) was added. The

reaction mixture was allowed to reach room temperature and stirred for 48 h. Solvent was evaporated and the mixture was dissolved in EtOAc (15 mL) and washed with 1M HCl (5 mL), a saturated solution of $NaHCO_3$ in H_2O (5 mL) and brine (5 mL). The water phase was extracted with EtOAc (3 × 10 mL). The combined organic phases were dried over Na_2SO_4, filtered and concentrated *in vacuo*. Beige solid, crude yield: 60 mg (148%). The crude product was purified with automated flash chromatography (DCM/MeOH 0→10 %) and then with preparative TLC (glass TLC plate, 100 % EtOAc). White solid, 21 mg (50 %). Melting point: 211-213°C. HRMS (ESI^+): calculated 594.9828 ($C_{22}H_{21}N_4O_6Br_2$), found 594.9825. LC-MS: [$M+H^+$] m/z 597 (t_R= 3.77 min), >99 %. ^1H NMR (400 MHz, d_6-DMSO) δ 8.61 (t, J = 5.8 Hz, 2H), 7.81 (s, 2H), 7.12 (d, J = 9.9 Hz, 2H), 6.22 (d, J = 9.9 Hz, 2H), 3.55 (s, 2H), 3.45 (s, 2H), 3.17 (d, J = 6.2 Hz, 4H), 1.52 – 1.44 (m, 4H). ^{13}C NMR (101 MHz, DMSO) δ 184.5, 158.5, 158.2, 155.1, 154.6, 146.8, 145.8, 128.0, 121.6, 85.2, 81.5, 43.4, 43.2, 38.5, 26.3. Graphic NMR spectra are included in Appendix 1.

6.3.11 General procedure for making acyl chloride from carboxylic acid (MS-4a, MS-11a, FV-3a):

7,9-dibromo-8-oxo-1-oxa-2-azaspiro[4.5]deca-2,6,9-triene-3-carboxylic acid (**MS.4**) (1 eq) was dissolved in anhydrous THF (2 mL) in a two-neck round-bottomed flask, then a catalytic amount (20 µL) of anhydrous DMF was added. Oxalyl chloride (1.5 eq) was added dropwise and the reaction was stirred at room temperature for 1.5 h. The solvent was removed under reduced pressure and the residue was taken up in the appropriate solvent as used directly in the next step.

6.3.12 tert-butyl (3-(7,9-dibromo-8-oxo-1-oxa-2-azaspiro[4.5]deca-2,6,9-triene-3-carboxamido)propyl)carbamate (MS-20)

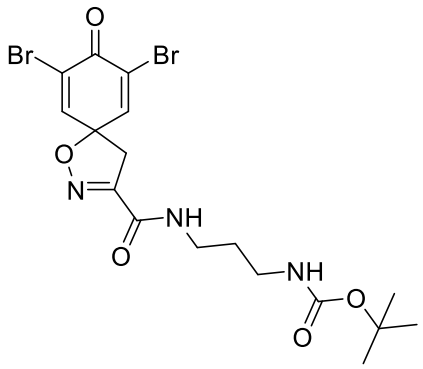

Et_3N (119 µL, 0.9 mmol, 3 eq.) was added to a solution of *N*-Boc-1,3-diaminopropane (65 mg, 0.4 mmol, 1.3 eq) in anhydrous DCM (2 mL) in a two-neck round-bottomed flask (amine dissolved completely after Et_3N was added). Then **MS-4a** (1 eq) was added dropwise in a mixture of DCM and THF (1:1, 8 mL). The mixture was stirred for 21 hours at room temperature, after that the solvent was removed in *vacuo*. The crude product (brown solid, 340 mg) was purified with automated flash chromatography (heptane/EtOAc 0→100 %). Yellow solid, 120 mg (83 %). APCI-MS: $[M-H]^-$ m/z 506. ^1H NMR (400 MHz, $CDCl_3$) δ 7.31 (s, 2H), 3.47 (s, 2H), 3.42 (dd, J = 12.7, 6.4 Hz, 2H), 3.25 – 3.16 (m, 2H), 1.74 – 1.65 (m, 2H), 1.45 (s, 9H). ^{13}C NMR (101 MHz, $CDCl_3$) δ 171.8, 158.8, 157.1, 154.3, 144.9, 124.1, 86.2, 80.1, 43.6, 37.7, 36.8, 30.6, 28.8.

6.3.13tert-butyl (3-(8-oxo-1-oxa-2-azaspiro[4.5]deca-2,6,9-triene-3-carboxamido)propyl)carbamate (MS-24)

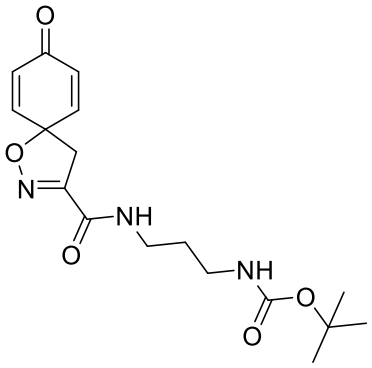

Et_3N (650 µL, 4.7 mmol, 3 eq.) was added to a solution of *N*-Boc-1,3-diaminopropane (350 mg, 2.0 mmol, 1.3 eq) in anhydrous DCM (2 mL) in a two-neck round-bottomed flask (amine dissolved completely after Et_3N was added). Then **MS-11a** (1 eq) was added dropwise in anhydrous THF (10 mL). The mixture was stirred for 21 hours at room temperature, after that the solvent was removed in *vacuo*. The crude product was purified with automated flash chromatography (heptane/EtOAc 20→100 %). White solid, 240 mg (44 %). APCI-MS: $[M-H]^-$ m/z 348. ^1H NMR (400 MHz, $CDCl_3$) δ 7.32 (s, 2H), 6.85 – 6.78 (m, 2H), 6.24 – 6.18 (m, 2H), 5.00 (t, J = 6.2 Hz, 2H), 3.39 – 3.33 (m, 2H), 3.18 – 3.07 (m, 2H), 1.71 – 1.61 (m, 2H), 1.36 (s, 2H). ^{13}C NMR (101 MHz, $CDCl_3$) δ 171.8, 158.8, 157.1, 154.3, 144.9, 124.1, 86.2, 80.1, 43.6, 37.7, 36.8, 30.6, 28.8.

6.3.14 N,N'-(propane-1,3-diyl)bis(8-oxo-1-oxa-2-azaspiro[4.5]deca-2,6,9-triene-3-carboxamide) (MS-30)

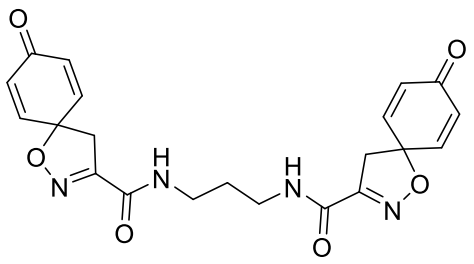

Et_3N (96 µL, 0.7 mmol, 3 eq.) was added to a solution of **MS-26** (60 mg, 0.2 mmol, 1 eq) in anhydrous DCM (2 mL) in a two-neck round-bottomed flask. Then **MS-11a** (1.3 eq) was added dropwise in anhydrous THF (5 mL). The mixture was stirred for 21 hours at room temperature, after that the solvent was removed in *vacuo*. Brown solid, 0.29 g). The crude product was purified with automated flash chromatography (heptane/EtOAc 45→100 %). White solid, 43 mg (44 %). Melting point: 192.5-193.5°C. HRMS (ESI^+): calculated 425.1461 ($C_{21}H_{21}N_4O_6$), found 425.1458. LC-MS: [$M+H^+$] m/z 425 (t_R= 2.26 min), >99 %. ^1H NMR (400 MHz, CD_3CN) δ 7.40 (s, 2H), 7.01 – 6.93 (m, 4H), 6.24 – 6.16 (m, 4H), 3.38 (s, 4H), 3.35 (q, J = 6.5 Hz, 4H), 1.74 (tt, J = 7.1, 6.1 Hz, 2H). ^{13}C NMR (101 MHz, CD_3CN) δ 185.5, 160.1, 155.4, 145.9, 129.3, 83.3, 44.3, 37.1, 30.0. Graphic NMR spectra are included in Appendix 1.

6.3.15 N-(3-(7,9-dichloro-8-oxo-1-oxa-2-azaspiro[4.5]deca-2,6,9-triene-3-carboxamido)propyl)-8-oxo-1-oxa-2-azaspiro[4.5]deca-2,6,9-triene-3-carboxamide (MS-31)

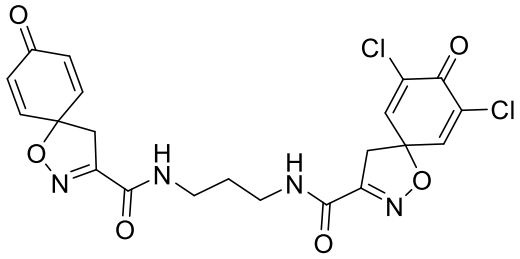

Et_3N (96 µL, 0.7 mmol, 3 eq.) was added to a solution of **MS-26** (60 mg, 0.2 mmol, 1 eq) in anhydrous DCM (2 mL) in a two-neck round-bottomed flask. Then **FV-3a** (1.3 eq) was added dropwise in anhydrous THF (10 mL). The mixture was stirred for 21 hours at room temperature, after that the solvent was removed in *vacuo*. Yellow solid, 330 mg). The crude product was purified with automated flash chromatography

(heptane/EtOAc 40→100 %). White solid, 40 mg (35 %). Melting point: 194.5–196.5°C. HRMS (ESI^+): calculated 493.0682 ($C_{21}H_{19}N_4O_6Cl_2$), found 493.0683. LC-MS: [$M+H^+$] m/z 493 (t_R= 3.46 min), >99 %. ^1H NMR (400 MHz, d_6-Acetone) δ 7.86 (t, J = 9.1 Hz, 2H), 7.48 (s, 2H), 7.12 – 7.07 (m, 2H), 6.24 – 6.18 (m, 2H), 3.67 (s, 2H), 3.49 (s, 2H), 3.41 (qd, J = 6.3, 1.6 Hz, 4H), 1.82 (p, J = 6.5 Hz, 2H). ^{13}C NMR (101 MHz, d_6-Acetone) δ 185.0, 172.7, 159.9, 159.6, 155.8, 155.3, 145.9, 142.7, 132.5, 129.2, 85.0, 83.1, 44.4, 44.3, 37.38, 37.35, 30.2. Graphic NMR spectra are included in Appendix 1.

6.4 Biological activity

The prepared compounds were tested for their antimycobacterial activity using minimum duration for killing (MDK) assay. The compounds were also tested for their potential synergistic effect with first-line drug rifampicin. The assay was performed by Lauri Paulamäki (PhD student) under the supervision of Associate Professor Mataleena Parikka at the Faculty of Medicine and Health Technology, University of Tampere, Finland.

Mycobacterium marinum Lux-reporter strain (ATCC927, American Type Culture Collection) was inoculated onto Middlebrook 7H10 agar (Becton, Dickinson and Company; Franklin Lakes, New Jersey, United States) culture plates and incubated at 28.5°C for 7 days. Bacterial culture was then transferred to Middlebrook 7H9 medium (Becton, Dickinson and Company; Franklin Lakes, New Jersey, United States) and diluted to OD_{600}: 0.1. The culture was then transferred to white opaque 96-well plates (CulturPlate-96, Perkin Elmer (Waltham, Massachusetts, USA)) 188 µl per well and incubated in 28.5°C for 7 days. Luminescence baseline was measured from each well with Perkin Elmer Envision plate reader. Lyophilized compounds used in the experiment were dissolved into 15 mM concentration in DMSO (Sigma-Aldrich, Schnelldorf, Germany). 6 µl of each compound was added to the wells with 8 µl of 10 mM rifampicin (Toku-E, Singapore) in sterilized water, three replicates of each. In addition, 6 µl of each compound was added with 8 µl of sterilized water. For control samples, 8 µl of 10 mM rifampicin was added with 6 µl of DMSO. Luminescence readings were measured every 24 h for 5 days.

Raw data was analyzed using R-4.1.0. programming language with in-house pipeline that parse the data and performs statistical testing. Readings of each well was normalized to the baseline luminescence and Area Under the Curve (AUC) value was calculated excluding the first data point. Each sample group was then compared using ANOVA. The graphs for each compound with untreated samples and control samples were drawn with ggplot2 package.

The results are shown in **Figures 21 – 23:**

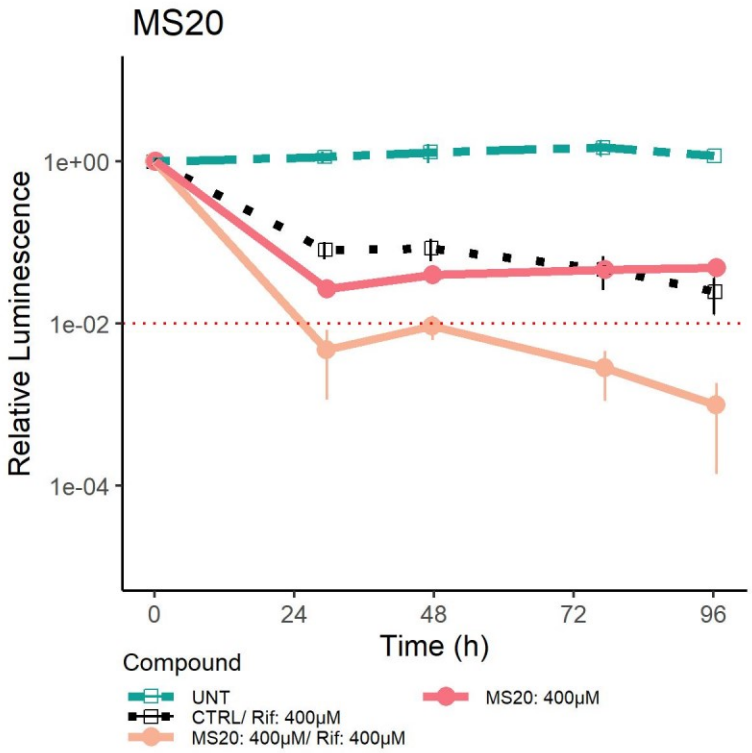

Figure 21: Antimycobacterial activity of the compound **MS-20**, described as a decline of relative luminiscence. UNT means untreated mycobacterial culture, thus without tested compound or any antibiotics. CTRL/Rif describes culture treated with rifampicin as a control sample.

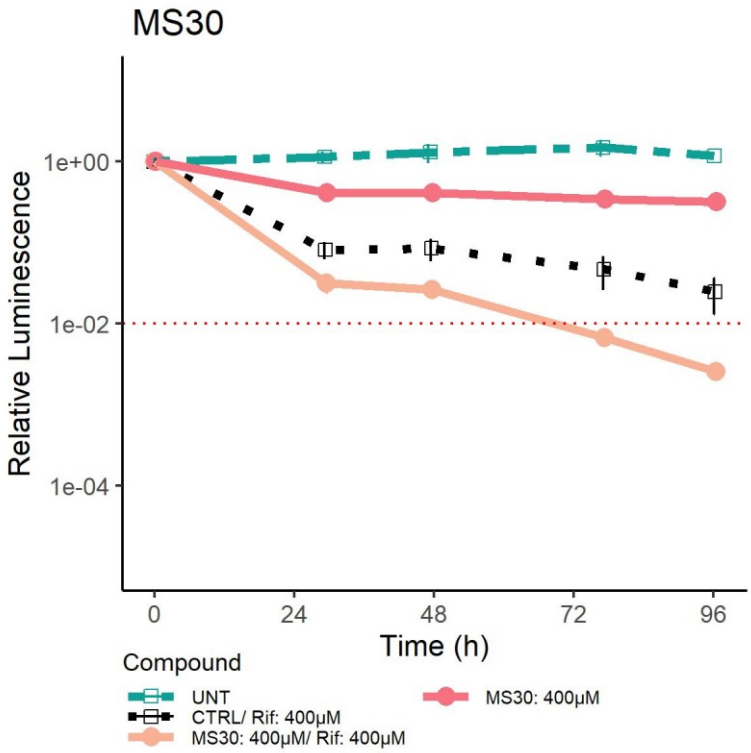

Figure 22: Antimycobacterial activity of the compound **MS-30**, described as a decline of relative luminiscence.

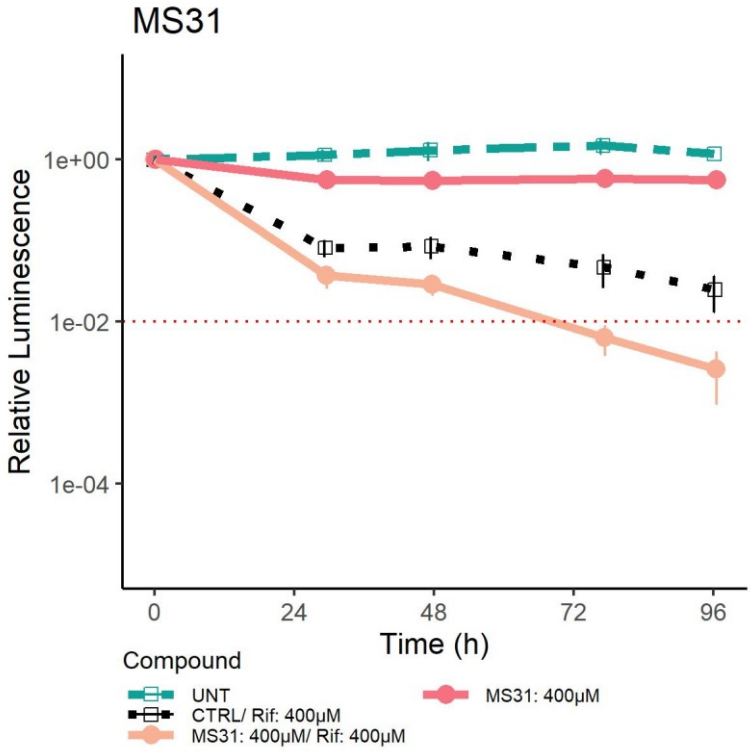

Figure 23: Antimycobacterial activity of the compound **MS-31**, described as a decline of relative luminiscence.

7 DISCUSSION AND CONCLUSIONS

Within this research work, three final products (**MS-22**, **MS-30** and **MS-31**) were synthesized through six-step synthesis. From seventeen synthesized compounds (products and intermediates), six were previously described in literature (**MS-1, MS-2, MS-3, MS-4, MS-9, MS-11**) and eleven were new, previously not described (**MS-15, MS-16, MS-17, MS-19, MS-20, MS-22, MS-23, MS-24, MS-26, MS-30, MS-31**) (SciFinder, 11th August 2020). The prepared final compounds and their purity were confirmed by 2D-NMR spectroscopy and high resolution mass spectrometry (HR-MS) and characterized by their melting point. (Graphic NMR spectra are included in Appendix 1.) At first, we were attempting to achieve the desired diamide products via one-step amide couplings. However, these procedures did not lead to the expected results. After many failures, creating one amide bond at a time turned out to be a better strategy, although these procedures also failed several times. Generally, from all the synthetic approaches only two were successful: coupling using HOBt/EDC while cooling (synthesis of product **MS-22**), and coupling using acyl chlorides (products **MS-30** and **MS-31**). For better comparison of these two methods, yields are listed in **Table 2**:

Table 2: Yields of the successful coupling methods.

Compound code	Method A (HOBt + EDC·HCl)	Method B (acyl chlorides)
MS-15	26 %	60 %
MS-16	17 %	
MS-20		83 %
MS-22	50 %	
MS-24		44 %
MS-30		44 %
MS-31		35 %

Even though intermediate compounds were not 100% pure it was obvious that forming amide bond through acyl chlorides leads to higher yields than HOBt/EDC mediated coupling and showed the way for the following syntheses. On the other hand, the performed reactions created questions that has yet to be answered:

- Why all the aerothionin synthetic methods described in the literature failed. At first, we assumed that it was because of the presence of TFA in the starting material, that could disrupt the amide coupling, but this assumption was refuted by unsuccessful reactions performed in the presence of neutralizing bases such as DIPEA or Et_3N.
- Why the reactions aiming at derivatives brominated on both sides failed at the final step, even though we managed to synthesize bromo-substituted intermediates, and also successfully performed coupling of brominated carboxylic acid on non-substitued intermediate.

Unfortunately, due to a limited time, we could not carry out more research to answer these questions and optimize the synthesis any further.

The three synthesized products were sent to *in vitro* antimycobacterial testing together with compound **MS-20**, which was the only mono-substituted intermediate obtained in sufficient purity (>99 %). Unfortunately, **MS-22** was not soluble enough to achieve desired 15 mM concentration in DMSO, so it could not be tested by the selected method.

Suprisingly, **MS-20** showed the best results in biological testing, as we can see in **Figure 21**. **MS-20** in combination with rifampicin decreased the luminiscence under 1 % of the initial value before 24 h. Slight increase in luminescence was observed in 48 h timepoint, yet the luminescence still stayed under 1 %. Without rifampicin, the killing efficiency was on par with rifampicin control treatment, which suggest direct cytotoxic effect. However, the antimycobacterial activity of **MS-20** should be verified using CFU-plating, to rule out possible direct luminescence quenching effect.

MS-30 was slower to take effect in combination with rifampicin, than the **MS-20**, although it reached the 1 % threshold at 72 h mark. Without antibiotics **MS-30** was less effective than the rifampicin control, although differed from untreated samples, suggesting lesser cytotoxic effect than **MS-20**.

MS-31 was similar in effect in comparison to **MS-30**, with only difference being lesser cytotoxic without rifampicin.

From these results we can assume that molecular dimer is not necessary for the activity of these derivatives. **MS-20** is active even though it lacks hydroxylation at position 1

and methoxy substitution at position 3 compared to aerothionin. On the other hand, compounds **MS-30** and **MS-31** were not very effective, which implies that bromination is probably one of the key components for the activity.

Results of this work encourage future research of these compounds. Optimization of the synthetic process is necessary, together with design and synthesis of new structures for further development of the most promising compound **MS-20**. It would be interesting to find out if only one bromine substitution would be sufficient, or whether the 3-[(*tert*-butoxycarbonyl)amino]propyl group could be replaced with simpler alkyl moiety. However, the fact that only one amide coupling will be needed, makes the synthesis and its optimization more aspicious for future scientists.

8 REFERENCES

(1) Peng, J.; Li, J.; Hamann, M. T. The Marine Bromotyrosine Derivatives. In *Alkaloids: Chemistry and Biology*; Cordell Geoffrey A., Ed.; Academic Press, **2005**; Vol. 61, pp 59–262.

(2) el Sayed, K. A.; Bartyzel, P.; Shen, X.; Perry, T. L.; Zjawiony, J. K.; Hamann, M. T. Marine Natural Products as Antituberculosis Agents. *Tetrahedron* **2000**, *56* (7), 949–953. https://doi.org/10.1016/S0040-4020(99)01093-5.

(3) de Oliveira, M. F.; de Oliveira, J. H.; Galetti, F. C.; de Souza, A. O.; Silva, C. L.; Hajdu, E.; Peixinho, S.; Berlinck, R. G. Antimycobacterial Brominated Metabolites from Two Species of Marine Sponges. *Planta Medica* **2006**, *72* (5), 437–441. https://doi.org/10.1055/s-2005-916239.

(4) Nicholas, M. , G.; Newton, L. , G.; Fahey, C. , R.; Bewley, A. C. Novel Bromotyrosine Alkaloids: Inhibitors of Mycothiol S-Conjugate Amidase. *Organic Letters* **2001**, *3* (10), 1543–1545.

(5) Encarnación-Dimayuga, R.; Ramírez, M. R.; Luna-Herrera, J. Aerothionin, a Bromotyrosine Derivative with Antimycobacterial Activity from the Marine Sponge *Aplysina gerardogreeni* (Demospongia). *Pharmaceutical Biology* **2003**, *41* (5), 384–387. https://doi.org/10.1076/phbi.41.5.384.15946.

(6) World Health Organisation. Global Tuberculosis Report 2020. https://apps.who.int/iris/bitstream/handle/10665/336069/9789240013131-eng.pdf (accessed Mar 14, 2021).

(7) Lawn, S. D.; Zumla, A. I. Tuberculosis. In *The Lancet*; Elsevier B.V., 2011; Vol. 378, pp 57–72. https://doi.org/10.1016/S0140-6736(10)62173-3.

(8) McMurray, D. N. Mycobacteria and Nocardia. In *Medical Microbiology*; Baron S., Ed.; University of Texas Medical Branch at Galveston: Galveston, **1996**. Chapter 33. Available from: https://www.ncbi.nlm.nih.gov/books/NBK7812/

(9) Akram, S. M.; Aboobacker, S. *Mycobacterium marinum* https://www.ncbi.nlm.nih.gov/books/NBK441883/ (accessed Aug 1, 2021).

(10) Petrini, B. *Mycobacterium marinum*: Ubiquitous Agent of Waterborne Granulomatous Skin Infections. *European Journal of Clinical Microbiology &*

Infectious Diseases **2006**, *25* (10), 609–613. https://doi.org/10.1007/s10096-006-0201-4.

(11) Prouty, M. G.; Correa, N. E.; Barker, L. P.; Jagadeeswaran, P.; Klose, K. E. Zebrafish- *Mycobacterium Marinum* Model for Mycobacterial Pathogenesis. *FEMS Microbiology Letters* **2003**, *225* (2), 177–182. https://doi.org/10.1016/S0378-1097(03)00446-4.

(12) Bloom, B. R.; Atun, R.; Cohen, T.; Dye, C.; Fraser, H.; Gomez, G. B.; Knight, G.; Murray, M.; Nardell, E.; Rubin, E.; Salomon, J.; Vassall, A.; Volchenkov, G.; White, R.; Wilson, D.; Yadav, P. Tuberculosis. In *Disease Control Priorities. Major Infectious Diseases.*; Holmes King K., Bertozzi Stefano, Bloom Barry R., Jha Prabhat, Eds.; The World Bank: Washington DC, 2017; Vol. 6, pp 233–293. https://doi.org/10.1596/978-1-4648-0524-0_ch11.

(13) Houben, R. M. G. J.; Dodd, P. J. The Global Burden of Latent Tuberculosis Infection: A Re-Estimation Using Mathematical Modelling. *PLOS Medicine* **2016**, *13* (10): e1002152. https://doi.org/10.1371/journal.pmed.1002152.

(14) Kiazyk, S.; Ball, T. Latent Tuberculosis Infection: An Overview. *Canada Communicable Disease Report* **2017**, *43* (3/4), 62–66. https://doi.org/10.14745/ccdr.v43i34a01.

(15) Gao, Y.; Liu, M.; Chen, Y.; Shi, S.; Geng, J.; Tian, J. Association between Tuberculosis and COVID-19 Severity and Mortality: A Rapid Systematic Review and Meta-analysis. *Journal of Medical Virology* **2021**, *93* (1), 194–196. https://doi.org/10.1002/jmv.26311.

(16) World Health Organisation. Implementing the end TB strategy: the essentials. https://www.who.int/teams/global-tuberculosis-programme/the-end-tb-strategy (accessed Jul 7, 2021).

(17) Maiolini, M.; Gause, S.; Taylor, J.; Steakin, T.; Shipp, G.; Lamichhane, P.; Deshmukh, B.; Shinde, V.; Bishayee, A.; Deshmukh, R. R. The War against Tuberculosis: A Review of Natural Compounds and Their Derivatives. *Molecules* **2020**, *25* (13): 3011. https://doi.org/10.3390/molecules25133011.

(18) World Health Organisation. Guidelines for treatment of tuberculosis. https://apps.who.int/iris/bitstream/handle/10665/44165/9789241547833_eng.pdf (accessed Mar 14, 2021).

(19) Roberts, C. Tuberculosis: A Multidisciplinary Approach to Past and Current Concepts, Causes and Treatment of This Infectious Disease. *Practitioners, Practices and Patients: new approaches to medical archaeology and anthropology*. Oxbow Books: Oxford 2002, pp 30–46.

(20) Grace, A. G.; Mittal, A.; Jain, S.; Tripathy, J. P.; Satyanarayana, S.; Tharyan, P.; Kirubakaran, R. Shortened Treatment Regimens versus the Standard Regimen for Drug-Sensitive Pulmonary Tuberculosis. *Cochrane Database of Systematic Reviews* **2018**, *12* (1). Art. No.: CD012918. https://doi.org/10.1002/14651858.CD012918.

(21) Farah, S. I.; Abdelrahman, A. A.; North, E. J.; Chauhan, H. Opportunities and Challenges for Natural Products as Novel Antituberculosis Agents. *ASSAY and Drug Development Technologies* **2016**, *14* (1), 29–38. https://doi.org/10.1089/adt.2015.673.

(22) World Health Organisation. Fact sheets. Antibiotic resistance. https://www.who.int/news-room/fact-sheets/detail/antibiotic-resistance (accessed Jul 31, 2021).

(23) Ventola, C. L. The Antibiotic Resistance Crisis: Part 1: Causes and Threats. *P & T : a peer-reviewed journal for formulary management* **2015**, *40* (4), 277–283.

(24) Walter, N. D.; Dolganov, G. M.; Garcia, B. J.; Worodria, W.; Andama, A.; Musisi, E.; Ayakaka, I.; Van, T. T.; Voskuil, M. I.; de Jong, B. C.; Davidson, R. M.; Fingerlin, T. E.; Kechris, K.; Palmer, C.; Nahid, P.; Daley, C. L.; Geraci, M.; Huang, L.; Cattamanchi, A.; Strong, M.; Schoolnik, G. K.; Davis, J. L. Transcriptional Adaptation of Drug-Tolerant *Mycobacterium tuberculosis* During Treatment of Human Tuberculosis. *Journal of Infectious Diseases* **2015**, *212* (6), 990–998. https://doi.org/10.1093/infdis/jiv149.

(25) Goossens, S. N.; Sampson, S. L.; van Rie, A. Mechanisms of Drug-Induced Tolerance in *Mycobacterium Tuberculosis*. *Clinical Microbiology Reviews* **2020**, *34* (1): e00141-20. https://doi.org/10.1128/CMR.00141-20.

(26) Jarlier, V.; Nikaido, H. Mycobacterial Cell Wall: Structure and Role in Natural Resistance to Antibiotics. *FEMS Microbiology Letters* **1994**, *123* (1–2), 11–18. https://doi.org/10.1111/j.1574-6968.1994.tb07194.x.

(27) Wiuff, C.; Zappala, R. M.; Regoes, R. R.; Garner, K. N.; Baquero, F.; Levin, B. R. Phenotypic Tolerance: Antibiotic Enrichment of Noninherited Resistance in Bacterial Populations. *Antimicrobial Agents and Chemotherapy* **2005**, *49* (4), 1483–1494. https://doi.org/10.1128/AAC.49.4.1483-1494.2005.

(28) Torrey, H. L.; Keren, I.; Via, L. E.; Lee, J. S.; Lewis, K. High Persister Mutants in Mycobacterium Tuberculosis. *PLOS ONE* **2016**, *11* (5): e0155127. https://doi.org/10.1371/journal.pone.0155127.

(29) Balouiri, M.; Sadiki, M.; Ibnsouda, S. K. Methods for in Vitro Evaluating Antimicrobial Activity: A Review. *Journal of Pharmaceutical Analysis* **2016**, *6* (2), 71–79. https://doi.org/10.1016/j.jpha.2015.11.005.

(30) Rios, J. L.; Recio, M. C.; Villar, A. Screening Methods for Natural Products with Antimicrobial Activity: A Review of the Literature. *Journal of Ethnopharmacology* **1988**, *23* (2–3), 127–149. https://doi.org/10.1016/0378-8741(88)90001-3.

(31) EUCAST. Antimicrobial susceptibility testing: EUCAST disk diffusion method https://www.eucast.org/ast_of_bacteria/disk_diffusion_methodology/ (accessed Jul 19, 2021).

(32) Sánchez, J. G. B.; Kouznetsov, V. v. Antimycobacterial Susceptibility Testing Methods for Natural Products Research. *Brazilian Journal of Microbiology* **2010**, *41* (2), 270–277. https://doi.org/10.1590/S1517-83822010000200001.

(33) Chung, G. A.; Aktar, Z.; Jackson, S.; Duncan, K. High-Throughput Screen for Detecting Antimycobacterial Agents. *Antimicrobial Agents and Chemotherapy* **1995**, *39* (10), 2235–2238. https://doi.org/10.1128/AAC.39.10.2235.

(34) Andreu, N.; Fletcher, T.; Krishnan, N.; Wiles, S.; Robertson, B. D. Rapid Measurement of Antituberculosis Drug Activity in Vitro and in Macrophages Using Bioluminescence. *Journal of Antimicrobial Chemotherapy* **2012**, *67* (2), 404–414. https://doi.org/10.1093/jac/dkr472.

(35) Picot, J.; Guerin, C. L.; le Van Kim, C.; Boulanger, C. M. Flow Cytometry: Retrospective, Fundamentals and Recent Instrumentation. *Cytotechnology* **2012**, *64* (2), 109–130. https://doi.org/10.1007/s10616-011-9415-0.

(36) Ballell, L.; Bates, R. H.; Young, R. J.; Alvarez-Gomez, D.; Alvarez-Ruiz, E.; Barroso, V.; Blanco, D.; Crespo, B.; Escribano, J.; González, R.; Lozano, S.; Huss, S.; Santos-Villarejo, A.; Martín-Plaza, J. J.; Mendoza, A.; Rebollo-Lopez, M. J.; Remuiñan-Blanco, M.; Lavandera, J. L.; Pérez-Herran, E.; Gamo-Benito, F. J.; García-Bustos, J. F.; Barros, D.; Castro, J. P.; Cammack, N. Fueling Open-Source Drug Discovery: 177 Small-Molecule Leads against Tuberculosis. *ChemMedChem* **2013**, *8* (2), 313–321. https://doi.org/10.1002/cmdc.201200428.

(37) Guardia, A.; Baiget, J.; Cacho, M.; Pérez, A.; Ortega-Guerra, M.; Nxumalo, W.; Khanye, S. D.; Rullas, J.; Ortega, F.; Jiménez, E.; Pérez-Herrán, E.; Fraile-Gabaldón, M. T.; Esquivias, J.; Fernández, R.; Porras-De Francisco, E.; Encinas, L.; Alonso, M.; Giordano, I.; Rivero, C.; Miguel-Siles, J.; Osende, J. G.; Badiola, K. A.; Rutledge, P. J.; Todd, M. H.; Remuiñán, M.; Alemparte, C. Easy-To-Synthesize Spirocyclic Compounds Possess Remarkable in Vivo Activity against *Mycobacterium tuberculosis*. *Journal of Medicinal Chemistry* **2018**, *61* (24), 11327–11340. https://doi.org/10.1021/acs.jmedchem.8b01533.

(38) Domenech, P.; Reed, M. B.; Barry, C. E. Contribution of the *Mycobacterium tuberculosis* MmpL Protein Family to Virulence and Drug Resistance. *Infection and Immunity* **2005**, *73* (6), 3492–3501. https://doi.org/10.1128/IAI.73.6.3492-3501.2005.

(39) Ray, P. C.; Huggett, M.; Turner, P. A.; Taylor, M.; Cleghorn, L. A. T.; Early, J.; Kumar, A.; Bonnett, S. A.; Flint, L.; Joerss, D.; Johnson, J.; Korkegian, A.; Mullen, S.; Moure, A. L.; Davis, S. H.; Murugesan, D.; Mathieson, M.; Caldwell, N.; Engelhart, C. A.; Schnappinger, D.; Epemolu, O.; Zuccotto, F.; Riley, J.; Scullion, P.; Stojanovski, L.; Massoudi, L.; Robertson, G. T.; Lenaerts, A. J.; Freiberg, G.; Kempf, D. J.; Masquelin, T.; Hipskind, P. A.; Odingo, J.; Read, K. D.; Green, S. R.; Wyatt, P. G.; Parish, T. Spirocycle MmpL3 Inhibitors with Improved HERG and Cytotoxicity Profiles as Inhibitors of *Mycobacterium tuberculosis* Growth. *ACS Omega* **2021**, *6* (3), 2284–2311. https://doi.org/10.1021/acsomega.0c05589.

(40) Badiola, K. A.; Quan, D. H.; Triccas, J. A.; Todd, M. H. Efficient Synthesis and Anti-Tubercular Activity of a Series of Spirocycles: An Exercise in Open Science. *PLoS ONE* **2014**, *9* (12): e111782. https://doi.org/10.1371/journal.pone.0111782.

(41) Cihan-Üstündağ, G.; Naesens, L.; Şatana, D.; Erköse-Genç, G.; Mataracı-Kara, E.; Çapan, G. Design, Synthesis, Antitubercular and Antiviral Properties of New Spirocyclic Indole Derivatives. *Monatshefte für Chemie - Chemical Monthly* **2019**, *150* (8), 1533–1544. https://doi.org/10.1007/s00706-019-02457-9.

(42) Cihan-Üstündağ, G.; Çapan, G. Synthesis and Evaluation of Functionalized Indoles as Antimycobacterial and Anticancer Agents. *Molecular Diversity* **2012**, *16* (3), 525–539. https://doi.org/10.1007/s11030-012-9385-y.

(43) Zhang, G.; Howe, M.; Aldrich, C. C. Spirocyclic and Bicyclic 8-Nitrobenzothiazinones for Tuberculosis with Improved Physicochemical and Pharmacokinetic Properties. *ACS Medicinal Chemistry Letters* **2019**, *10* (3), 348–351. https://doi.org/10.1021/acsmedchemlett.8b00634.

(44) Makarov, V.; Lechartier, B.; Zhang, M.; Neres, J.; Sar, A. M.; Raadsen, S. A.; Hartkoorn, R. C.; Ryabova, O. B.; Vocat, A.; Decosterd, L. A.; Widmer, N.; Buclin, T.; Bitter, W.; Andries, K.; Pojer, F.; Dyson, P. J.; Cole, S. T. Towards a New Combination Therapy for Tuberculosis with next Generation Benzothiazinones. *EMBO Molecular Medicine* **2014**, *6* (3), 372–383. https://doi.org/10.1002/emmm.201303575.

(45) Krasavin, M.; Lukin, A.; Vedekhina, T.; Manicheva, O.; Dogonadze, M.; Vinogradova, T.; Zabolotnykh, N.; Rogacheva, E.; Kraeva, L.; Sharoyko, V.; Tennikova, T. B.; Dar'in, D.; Sokolovich, E. Attachment of a 5-Nitrofuroyl Moiety to Spirocyclic Piperidines Produces Non-Toxic Nitrofurans That Are Efficacious in Vitro against Multidrug-Resistant Mycobacterium Tuberculosis. *European Journal of Medicinal Chemistry* **2019**, *166*, 125–135. https://doi.org/10.1016/j.ejmech.2019.01.050.

(46) Daletos, G.; Ancheeva, E.; Chaidir, C.; Kalscheuer, R.; Proksch, P. Antimycobacterial Metabolites from Marine Invertebrates. *Archiv der Pharmazie* **2016**, *349* (10), 763–773. https://doi.org/10.1002/ardp.201600128.

(47) García-Vilas, J.; Martínez-Poveda, B.; Quesada, A.; Medina, M. Aeroplysinin-1, a Sponge-Derived Multi-Targeted Bioactive Marine Drug. *Marine Drugs* **2015**, *14* (1): 1. https://doi.org/10.3390/md14010001.

(48) Niemann, H.; Marmann, A.; Lin, W.; Proksch, P. Sponge Derived Bromotyrosines: Structural Diversity through Natural Combinatorial Chemistry. *Natural Product Communications* **2015**, *10* (1), 219–231. https://doi.org/10.1177/1934578X1501000143.

(49) Mayer, A. M. S.; Guerrero, A. J.; Rodríguez, A. D.; Taglialatela-Scafati, O.; Nakamura, F.; Fusetani, N. Marine Pharmacology in 2014–2015: Marine Compounds with Antibacterial, Antidiabetic, Antifungal, Anti-Inflammatory, Antiprotozoal, Antituberculosis, Antiviral, and Anthelmintic Activities; Affecting the Immune and Nervous Systems, and Other Miscellaneous Mechanisms of Action. *Marine Drugs* **2019**, *18* (1): 3011. https://doi.org/10.3390/md18010005.

(50) Murali Krishna Kumar, M.; Devilal Naik, J.; Satyavathi, K.; Ramana, H.; Raghuveer Varma, P.; Purna Nagasree, K.; Smitha, D.; Venkata Rao, D. Denigrins A–C: New Antitubercular 3,4-Diarylpyrrole Alkaloids from *Dendrilla nigra*. *Natural Product Research* **2014**, *28* (12), 888–894. https://doi.org/10.1080/14786419.2014.891112.

(51) Daletos, G.; Kalscheuer, R.; Koliwer-Brandl, H.; Hartmann, R.; de Voogd, N. J.; Wray, V.; Lin, W.; Proksch, P. Callyaerins from the Marine Sponge *Callyspongia aerizusa* : Cyclic Peptides with Antitubercular Activity. *Journal of Natural Products* **2015**, *78* (8), 1910–1925. https://doi.org/10.1021/acs.jnatprod.5b00266.

(52) Arai, M.; Sobou, M.; Vilchéze, C.; Baughn, A.; Hashizume, H.; Pruksakorn, P.; Ishida, S.; Matsumoto, M.; Jacobs, W. R.; Kobayashi, M. Halicyclamine A, a Marine Spongean Alkaloid as a Lead for Anti-Tuberculosis Agent. *Bioorganic & Medicinal Chemistry* **2008**, *16* (14), 6732–6736. https://doi.org/10.1016/j.bmc.2008.05.061.

(53) Wei, X.; Nieves, K.; Rodríguez, A. D. Neopetrosiamine A, Biologically Active Bis-Piperidine Alkaloid from the Caribbean Sea Sponge *Neopetrosia proxima*.

Bioorganic & Medicinal Chemistry Letters **2010**, *20* (19), 5905–5908. https://doi.org/10.1016/j.bmcl.2010.07.084.

(54) Lin, Z.; Koch, M.; Abdel Aziz, M. H.; Galindo-Murillo, R.; Tianero, Ma. D.; Cheatham, T. E.; Barrows, L. R.; Reilly, C. A.; Schmidt, E. W. Oxazinin A, a Pseudodimeric Natural Product of Mixed Biosynthetic Origin from a Filamentous Fungus. *Organic Letters* **2014**, *16* (18), 4774–4777. https://doi.org/10.1021/ol502227x.

(55) Shen, X.; Perry, T. L.; Dunbar, C. D.; Kelly-Borges, M.; Hamann, M. T. Debromosceptrin, an Alkaloid from the Caribbean Sponge *Agelas conifera*. *Journal of Natural Products* **1998**, *61* (10), 1302–1303. https://doi.org/10.1021/np980129a.

(56) Vicente, J.; Vera, B.; Rodríguez, A. D.; Rodríguez-Escudero, I.; Raptis, R. G. Euryjanicin A: A New Cycloheptapeptide from the Caribbean Marine Sponge *Prosuberites laughlini*. *Tetrahedron Letters* **2009**, *50* (32), 4571–4574. https://doi.org/10.1016/j.tetlet.2009.05.067.

(57) Arai, M.; Yamano, Y.; Setiawan, A.; Kobayashi, M. Identification of the Target Protein of Agelasine D, a Marine Sponge Diterpene Alkaloid, as an Anti-Dormant Mycobacterial Substance. *ChemBioChem* **2014**, *15* (1), 117–123. https://doi.org/10.1002/cbic.201300470.

(58) Abou-Shoer, M. I.; Shaala, L. A.; Youssef, D. T. A.; Badr, J. M.; Habib, A.-A. M. Bioactive Brominated Metabolites from the Red Sea Sponge *Suberea mollis*. *Journal of Natural Products* **2008**, *71* (8), 1464–1467. https://doi.org/10.1021/np800142n.

(59) Fattorusso, E.; Minale, L.; Sodano, G.; Moody, K.; Thomson, R. H. Aerothionin, a Tetrabromo-Compound from *Aplysina aerophoba* and *Verongia thiona*. *Journal of the Chemical Society D: Chemical Communications* **1970**, No. 12, 752–753. https://doi.org/10.1039/c29700000752.

(60) Kernan, M. R.; Cambie, R. C.; Bergquist, P. R. Chemistry of Sponges, VII. 11,19-Dideoxyfistularin 3 and 11-Hydroxyaerothionin, Bromotyrosine Derivatives from *Pseudoceratina durissima*. *Journal of Natural Products* **1990**, *53* (3), 615–622. https://doi.org/10.1021/np50069a012.

(61) Ankudey, F.; Kiprof, P.; Stromquist, E.; Chang, L. New Bioactive Bromotyrosine-Derived Alkaloid from a Marine Sponge *Aplysinella* Sp. *Planta Medica* **2008**, *74* (5), 555–559. https://doi.org/10.1055/s-2008-1074506.

(62) Acosta, A. L.; Rodríguez, A. D. 11-Oxoaerothionin: A Cytotoxic Antitumor Bromotyrosine-Derived Alkaloid from the Caribbean Marine Sponge Aplysina Lacunosa. *Journal of Natural Products* **1992**, *55* (7), 1007–1012. https://doi.org/10.1021/np50085a031.

(63) Montalbetti, C. A. G. N.; Falque, V. Amide Bond Formation and Peptide Coupling. *Tetrahedron* **2005**, *61* (46), 10827–10852. https://doi.org/10.1016/j.tet.2005.08.031.

(64) Valeur, E.; Bradley, M. Amide Bond Formation: Beyond the Myth of Coupling Reagents. *Chem. Soc. Rev.* **2009**, *38* (2), 606–631. https://doi.org/10.1039/B701677H.

(65) Carpino, L. A. 1-Hydroxy-7-Azabenzotriazole. An Efficient Peptide Coupling Additive. *Journal of the American Chemical Society* **1993**, *115* (10), 4397–4398. https://doi.org/10.1021/ja00063a082.

(66) van den Nest, W.; Yuval, S.; Albericio, F. $Cu(OBt)_2$ and $Cu(OAt)_2$, Copper(II)-Based Racemization Suppressors Ready for Use in Fully Automated Solid-Phase Peptide Synthesis. *Journal of Peptide Science* **2001**, *7* (3), 115–120. https://doi.org/10.1002/psc.299.

(67) Carpino, L. A.; El-Faham, A.; Albericio, F. Racemization Studies during Solid-Phase Peptide Synthesis Using Azabenzotriazole-Based Coupling Reagents. *Tetrahedron Letters* **1994**, *35* (15), 2279–2282. https://doi.org/10.1016/0040-4039(94)85198-0.

(68) Albericio, F.; El-Faham, A. Choosing the Right Coupling Reagent for Peptides: A Twenty-Five-Year Journey. *Organic Process Research & Development* **2018**, *22* (7), 760–772. https://doi.org/10.1021/acs.oprd.8b00159.

(69) Moiola, M.; Memeo, M. G.; Quadrelli, P. Stapled Peptides—A Useful Improvement for Peptide-Based Drugs. *Molecules* **2019**, *24* (20): 3654. https://doi.org/10.3390/molecules24203654.

(70) Albericio, F.; Bofill, J. M.; El-Faham, A.; Kates, S. A. Use of Onium Salt-Based Coupling Reagents in Peptide Synthesis. *The Journal of Organic Chemistry* **1998**, *63* (26), 9678–9683. https://doi.org/10.1021/jo980807y.

(71) Clayden, J.; Greeves, N.; Warren, S.; Wothers, P. *Organic Chemistry*, 1st ed.; Oxford University Press, 2001; pp 214–215.

(72) Patel, P. A.; Bruun, T.; Ilina, P.; Mäkkylä, H.; Lempinen, A.; Yli-Kauhalouma, J.; Tammela, P.; Kiuru, P. S. Synthesis and Antiproliferative Evaluation of Spirocyclic Bromotyrosine Clavatadine-C Analogs. *Marine Drugs* **2021**, *19* (7). https://doi.org/10.3390/md19070400.

(73) Ogamino, T.; Nishiyama, S. Synthesis and Structural Revision of Calafianin, a Member of the Spiroisoxazole Family Isolated from the Marine Sponge, *Aplysina gerardogreeni*. *Tetrahedron Letters* **2005**, *46* (7), 1083–1086. https://doi.org/10.1016/j.tetlet.2004.12.084.

(74) García, J.; Pereira, R.; de Lera, A. R. Total Synthesis of the Natural Isoprenylcysteine Carboxyl Methyltransferase Inhibitor Spermatinamine. *Tetrahedron Letters* **2009**, *50* (35), 5028–5030. https://doi.org/10.1016/j.tetlet.2009.06.087.

(75) Nishiyama, S.; Yamamura, S. Total Syntheses of (±)-Aerothionin and (±)-Homoaerothionin. *Tetrahedron Letters* **1983**, *24* (32), 3351–3352. https://doi.org/10.1016/S0040-4039(00)86267-X.

(76) Kvasnica, M. Dicyclohexylcarbodiimide (DCC). *Synlett* **2007**, *2007* (14), 2306–2307. https://doi.org/10.1055/s-2007-985575.

(77) Parks, D. J.; Parsons, W. H.; Colburn, R. W.; Meegalla, S. K.; Ballentine, S. K.; Illig, C. R.; Qin, N.; Liu, Y.; Hutchinson, T. L.; Lubin, M. lou; Stone, D. J.; Baker, J. F.; Schneider, C. R.; Ma, J.; Damiano, B. P.; Flores, C. M.; Player, M. R. Design and Optimization of Benzimidazole-Containing Transient Receptor Potential Melastatin 8 (TRPM8) Antagonists. *Journal of Medicinal Chemistry* **2011**, *54* (1), 233–247. https://doi.org/10.1021/jm101075v.

(78) Mangum, C. L.; Munford, M. B.; Sam, A. B.; Young, S. K.; Beales, J. T.; Subedi, Y. P.; Mangum, C. D.; Allen, T. J.; Liddell, M. S.; Merrell, A. I.; Saavedra, D. I.; Williams, B. L.; Evans, N.; Beales, J. L.; Christiansen, M. A. The Total

Syntheses of JBIR-94 and Two Synthetic Analogs and Their Cytotoxicities against A549 (CCL-185) Human Small Lung Cancer Cells. *Tetrahedron Letters* **2020**, *61* (1), 151360. https://doi.org/10.1016/j.tetlet.2019.151360.